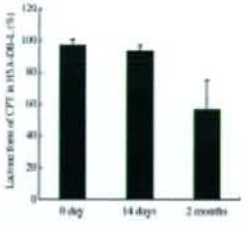

Fig. 3. Storage stability of lactone form of CPT incorporated in HSA-DB-L at room temperature. Each value represents the mean±SD. (n=3).

when the liposomes were prepared at a feeding ratio of 1/30 (w/w) CPT/total lipid (Table 1). The effect of PEG on the association of HSA was evaluated using HSA-DB-L with or without PEG2000. The adsorbed HSA amounts on HSA-DB-L (HSPC/Ch/OA/DB/PEG2000+HSA) and HSA-DB-L without PEG2000 (HSPC/Ch/OA/DB+HSA) was 58.7±5.3 and 73.3±6.5 mg HSA/g HSPC, respectively. The presence of PEG reduced the association of HSA on the surface of DB-L compared with DB-L without PEG2000. This finding was also confirmed by SDS-PAGE as shown in Fig. 2. HSA-DB-L was successfully modified with HSA by incubation.

Moreover, analysis of HSA-DB-L, i.e., DB-L coated with HSA, demonstrated that neither the particle size nor the incorporation efficiency was changed by incubation of the liposomes with HSA. The surface potentials of DB-L and HSA-DB-L were −23.1±2.0 mV and −26.3±5.4 mV, respectively.

Drug release profiles of Control-L and DB-L showed that there was approximately 30% drug release from CPT liposomes into PBS over 72 h (data not shown), suggesting the CPT remained associated with the liposomes during the course of the study. This finding also suggests that CPT liposomes would be stable in dilute conditions.

3.2. In vivo circulation stability of CPT liposomes

To determine whether CPT liposomes were stable and long circulating, the plasma concentration of CPT liposomes was evaluated 4 h after mice were injected intravenously (Table 1). DB-L, which contained DB in addition to the formulation of Control-L, showed a significantly (about 3-fold) higher level CPT in the plasma compared to Control-L ($P<0.05$). This suggests that the addition of DB in the liposome bilayer increased the stability of CPT-incorporating liposomes in the blood. However, changing the PEG length from 2000 to 5000 (DB-L5000) or the addition of a 2-fold larger amount of DB in DB-L (2DB-L) failed to increase the CPT plasma concentration, although both formulations showed similar particle size and incorporation efficiency as DB-L. The result suggests that the level of incorporation of DB influenced on the distribution of CPT in liposomes.

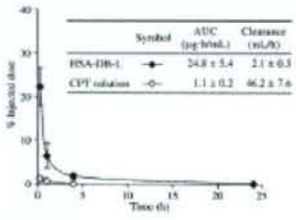

Fig. 4. Plasma concentration–time curves of the HSA-DB-L and CPT solution following i.v. injection at a dose of 2.5 mg CPT/kg in ddY mice. Each value represents the mean±SD. (n=3).

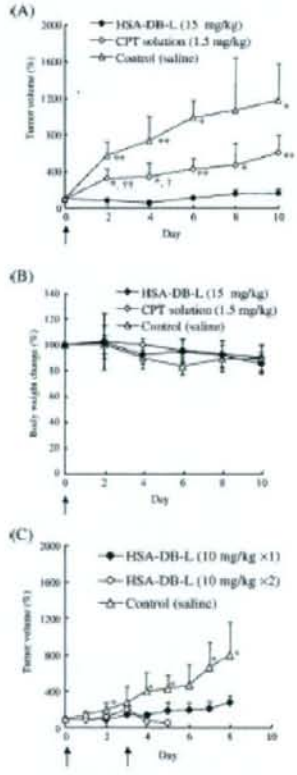

Fig. 5. In vivo antitumor activity in mice bearing C26 tumors. (A, B) Tumor volume and body weight change after a single injection of 15 mg/kg CPT in HSA-DB-L or 1.5 mg/kg CPT solution. (C) Single or repeated injection of 10 mg/kg CPT in HSA-DB-L. Arrows indicate the day of drug injections. Tumor volumes are plotted as ratios to their volume prior to the first drug injection. Each value represents the mean±S.D. ($n=4$) *$P<0.05$, **$P<0.01$ compared with HSA-DB-L, †$P<0.05$, ††$P<0.01$ compared with control.

It has been reported that pre-coating polystyrene particles with HSA enhanced their stability in blood [23]. To increase the circulation stability of DB-L, therefore, the surface of DB-L was coated with HSA (HSA-DB-L). HSA-DB-L showed significantly (about 2.5-fold) higher CPT plasma concentration than DB-L ($P<0.01$).

3.3. Storage stability of CPT liposomes

Generally, the carboxylate form of CPT binds with HSA and is changed to the pharmacologically ineffective carboxylate form [5]. Therefore, the storage stability of HSA-DB-L at room temperature was examined by measuring the amount of CPT lactone form remaining by HPLC. As shown in Fig. 3, more than 95% of the lactone form of CPT in HSA-DB-L remained 14 days after preparation ($P>0.05$), and more than 50% at 2 months compared with that on day 0 without change of the size/polydispersity index over time.

3.4. Plasma concentration–time profiles in mice

As shown above, CPT liposomes that were stable in the blood circulation and in storage were obtained using an appropriate formulation of CPT liposomes coated with HSA. Next, the plasma pharmacokinetics of the HSA-DB-L was compared with those of CPT solution in mice (Fig. 4). CPT solution disappeared very quickly from the blood circulation. The CPT in HSA-DB-L was clearly more stable in the blood circulation than CPT solution. The percentage of the injected dose of HSA-DB-L remaining in plasma 15 min, 1, and 4 h after injection was significantly (19.5-, 10.9-, and 44.5-fold, respectively) higher than that of CPT solution. The AUC values of HSA-DB-L and CPT solution were 24.8 and 1.1 μg·h/mL, respectively, and their clearance values were 2.1 and 46.2 mL/h, respectively. Thus, HSA-DB-L showed about 22-fold higher AUC and a 22-fold lower clearance values than CPT solution.

3.5. Efficacy of single or repeated administration of CPT liposomes in C26-bearing mice

The efficacy of a single i.v. injection of HSA-DB-L at a dose of 15 mg CPT/kg against the growth of C26 in tumor-bearing mice was evaluated by monitoring tumor growth (Fig. 5(A)). The dose of CPT liposomes was decided from data that CPT-loaded polymeric micelles showed the maximum dose was 30 mg/kg after a single i.v. administration to mice [12]. HSA-DB-L showed much higher antitumor activity than CPT solution or the saline control. Mice treated with CPT solution showed a significantly smaller tumor volume than control mice. The relative tumor volume (%) in HSA-DB-L-treated mice was significantly lower than that in mice treated with the saline control or CPT solution with treated/control (T/C) volume of 16.4% at Day 8. The mice treated with HSA-DB-L as a single i.v. injection at a dose of 15 mg CPT/kg did not show any significant body weight loss during the observation period (Fig. 5(B)). The dose of CPT solution used (1.5 mg CPT/kg) was 10-fold lower than that of HSA-DB-L. The dose could not be increased, because in preliminary experiments a higher dose (2.5 mg/kg) often resulted in death after i.v. injection. Thus, the antitumor treatment with HSA-DB-L would have yielded a higher plasma concentration of CPT, and this may have accounted for the larger antitumor effect than that of CPT solution.

In order to increase the efficacy of the treatment using HSA-DB-L, the administration schedule was changed to repeated injection using a decreased dose (10 mg/kg instead of 15 mg/kg) on Days 0 and 3 (Fig. 5(C)). A single injection of HSA-DB-L at a dose of 10 mg CPT/kg showed significant antitumor activity with T/C% of 34.6 at Day 8. Repeated injection of HSA-DB-L resulted in a body weight loss of approximately 20% on the third day after the second injection (data not shown), and within 2 more days, all of the treated mice died. This seemed to be related to CPT toxicity, because when empty HSA-DB-L (not containing CPT) was injected in mice on the same schedule as used in Fig. 5(C), no mice died (data not shown).

3.6. Biodistribution of CPT liposomes in tumor-bearing mice

Fig. 6(A) shows the amount of CPT in tissues of mice bearing C26 tumors, and Fig. 6(B) shows the percent of the dose of injected CPT in the blood 24 h after the injection of HSA-DB-L. Tumor tissue exposed to HSA-DB-L demonstrated significantly (9.6-fold) higher CPT accumulation than tumor tissue exposed to CPT solution ($P<0.05$). CPT accumulation of HSA-DB-L in liver and lung was decreased but that of kidneys was increased

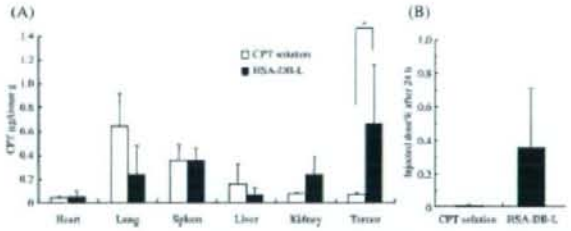

Fig. 6. Biodistribution of CPT 24 h after i.v. injection of HSA-DB-L or CPT solution (2.5 mg CPT/kg) into mice bearing C26. (A) Amount CPT per tissue weight. Each value represents the mean± S.D. ($n=3$) *: $P<0.05$ (B) % of injected dose of CPT in plasma. Each value represents the mean±S.E. ($n=3$).

by HSA-DB-L treatment ($P>0.05$). Furthermore, the plasma level of CPT in HSA-DB-L-treated mice remained 60-fold higher than that in mice treated with CPT solution.

4. Discussion

Stable pegylated liposome-incorporated CPT was obtained by the addition of DB to the formulation for liposomes combined with coating the surface of the liposomes with HSA. The CPT liposomes showed activity against C26 tumors resulting from high accumulation of CPT in the tumors when administered as a single i.v. injection in mice.

To improve the pharmacological usefulness of CPT, a liposomal formulation including CPT was developed, and the CPT liposomes were evaluated regarding their particle size, incorporation efficiency, drug release in vitro, and stability in vivo. Liposomes composed of HSPC and Ch showed low retention in the blood 4 h after injection (0.09% of injected dose of CPT). Addition of OA to the liposomes increased the retention of the injected dose of CPT to 0.4% (data not shown), suggesting that OA might increase the acidity of liposomes, resulting in stabilization of the lactone form of CPT.

All formulations demonstrated high incorporation efficiency (more than about 80%) when liposomes were prepared in acidic conditions (pH 6.0) (Table 1). This could be due to the fact that the stability of the lactone form of the CPT molecule is favored by lower pH conditions than the carboxylate form, which is more hydrophilic at pH 7.0 [29]. Among the formulations examined, DB-L (HSPC/Ch/OA/DB/PEG2000 7:3:1:1:0.4) was most stable after i.v. injection. At present, whether DB interacts with CPT is not clear, but we have reported that the stability of CPT-loaded polymeric micelles in vivo was increased by benzylesterification of the hydrophobic segment of the block copolymer [11], presumably due to be π–π interaction of the phenyl group with CPT. DB in liposome membranes, therefore, might interact with CPT by a π–π interaction and could incorporate CPT into the interior of the bilayers. However, 2DB-L, containing 15 mol% DB, decreased the CPT concentration in plasma compared to DB-L. This suggests that there is an optimal amount of DB for increasing the stability of CPT liposomes, which may be between 8 and 15 mol%. As mentioned above, CPT interacted with DB in liposomal membrane. The incorporation efficiency of DB in liposomes had optimal value. Thus, optimal amount of DB for increasing CPT stability may exist.

The association of some serum protein with opsonic activity has been suppressed in previous studies by pre-coating HSA on the surface of nanoparticles and nanospheres [23,30]. In accord with those observations, HSA-DB-L increased the stability of CPT in the circulation compared to liposomes without HSA on their surface. Carbonyl group of the ring D of CPT may be in liposomes and HSA coating may stabilize them.

CPT solution given as a single i.v. injection at 2.5 mg/kg in tumor-bearing mice often resulted in toxic death, but HSA-DB-L at 15 mg/kg did not cause any significant body weight loss. This finding suggests that HSA-DB-L was up to 6 times less toxic than CPT solution administered by i.v. injection. The pharmacokinetics and tissue distribution data indicated that this reduced toxicity was attributable to lower uptake of CPT in the liver and lung after treatment with HSA-DB-L than after the administration of an equimolar dose of CPT solution. Because of this reduced toxicity, a higher dose of CPT liposomes could be used to treat mice bearing murine colon cancer. HSA-DB-L with low clearance increased the accumulation of CPT in tumor tissue, resulting in increase of the antitumor effect of CPT.

Regarding the therapeutic strategy, it has been shown in nude mice bearing human tumor xenografts that for a fixed total dose, repeated daily administration of CPT conjugated with polymers was far superior to a single injection [31]. Here, our findings suggest that a single injection of HSA-DB-L was effective for suppressing tumor growth at a dose of either 10 or 15 mg/kg (T/C% = 34.6% and 16.4% at Day 8, respectively). This apparent discrepancy may be due to a difference in the rate of release of free CPT from the liposomes. Although CPT has been shown to be released slowly from CPT conjugated with polymers over several days [31,32], HSA-DB-L released about 20% of its load within 24 h from release test into PBS. These findings suggest that the rapid bioavailability of free CPT from the liposomes may indeed improve antitumor activity subsequent to the passive accumulation of liposomes in the tumor tissue.

DB was not cytotoxic, and therefore the antitumor effect of HSA-DB-L may have been due to CPT. Furthermore, we have synthesized DB derivatives and investigated the interaction between the dodecyloxy group of DB and the lactone ring of CPT to estimate the distribution of CPT in liposomes containing DB. These results were reported as separate manuscript [33].

The results from the biodistribution study revealed that the intravenously injected HSA-DB-L accumulated in the tumor. Drug carriers with a prolonged circulation time can increase the drug accumulation in tumor tissues by the EPR effect, and consequently improve the antitumor activity. Although pegylated liposome, HSA-DB-L seemed to contribute improved CPT solubility in lipids over long circulating, these results suggest that HSA-DB-L with stable property in blood possesses the ability to deliver large amounts of CPT to the tumor site. Here further studies with human tumor xenografts will be required to evaluate the activity of HSA-DB-L.

5. Conclusion

CPT liposomes formulated with DB increased the CPT stability in vitro and in vivo. Furthermore, CPT liposomes coated with HSA prolonged the blood circulation time. This formulation enhanced the accumulation of CPT in tumor tissue, resulting in a significantly higher antitumor effect than CPT solution even with a single injection. This finding will permit the utilization of CPT, which is not now used in clinical practice due to the lack of a suitable drug carrier system.

Acknowledgements

This study was supported in part by the Ministry of Education, Culture, Sports, Science and Technology, Japan, and by the Open Research Center Project. We are grateful to Ms. S. Katayama, Mr. C. Fujita and Ms. M. Katori for technical assistance.

References

[1] M.E. Wall, M.C. Wani, C.E. Cook, K.H. Palmer, A.T. Mcphail, G.A. Sim, Plant antitumor agents: I. The isolation and structure of camptothecin, a novel alkaloidal leukemia and tumor inhibitor from Camptotheca acuminate, J. Am. Chem. Soc. 88 (1966) 3888–3890.

[2] B.C. Giovanella, J.S. Stehlin, M.E. Wall, M.C. Wani, A.W. Nicholas, L.F. Liu, R. Silber, M. Potmesil, DNA topoisomerase I-targeted chemotherapy of human colon cancer in xenografts, Science 246 (1989) 1046–1048.

[3] B.C. Giovanella, H.R. Hinz, A.J. Kozielski, J.S. Stehlin Jr., R. Silber, M. Potmesil, Complete growth inhibition of human cancer xenografts in nude mice by treatment with 20-(S)-camptothecin, Cancer Res. 51 (1991) 3052–3055.

[4] R.P. Hertzberg, M.J. Caranfa, S.M. Hecht, On the mechanism of topoisomerase I inhibition by camptothecin: evidence for binding to an enzyme–DNA complex, Biochemistry 28 (1989) 4629–4638.

[5] J. Fassberg, V.J. Stella, A kinetic and mechanistic study of the hydrolysis of camptothecin and some analogues, J. Pharm. Sci. 81 (1992) 676–684.

[6] Z. Mi, T.G. Burke, Differential interactions of camptothecin lactone and carboxylate forms with human blood components, Biochemistry 33 (1994) 10325–10336.

[7] K. Akimoto, A. Kawai, K. Ohya, Kinetic studies of the hydrolysis and lactonization of camptothecin and its derivatives, CPT-11 and SN-38, in aqueous solution, Chem. Pharm. Bull. 42 (1994) 2135–2138.

[8] B.A. Hanson, R.L. Schowen, V.J. Stella, A mechanistic and kinetic study of the E-ring hydrolysis and lactonization of a novel phosphoryloxymethyl prodrug of camptothecin, Pharm. Res. 20 (2003) 1031–1038.

[9] T.G. Burke, A.R. Staubus, A.K. Mishra, Liposomal stabilization of camptothecin's lactone ring, J. Am. Chem. Soc. 114 (1992) 8318–8319.

[10] R. Cortesi, E. Esposito, A. Maietti, E. Menegatti, C. Nastruzzi, Formulation study for the antitumor drug camptothecin: liposomes, micellar solution, and a microemulsion, Int. J. Pharm. 159 (1997) 95–103.

[11] M. Watanabe, K. Kawano, M. Yokoyama, P. Opanasopit, T. Okano, Y. Maitani, Preparation of camptothecin-loaded polymeric micelles and evaluation of their incorporation and circulation stability, Int. J. Pharm. 308 (2006) 183–189.

[12] K. Kawano, M. Watanabe, T. Yamamoto, M. Yokoyama, P. Opanasopit, T. Okano, Y. Maitani, Enhanced anti-tumor effect of camptothecin loaded in long-circulating polymeric micelles, J. Control. Release 112 (2006) 329–332.

[13] A. Shenderova, T.G. Burke, S.P. Schwendeman, The acidic microclimate in poly(lactide-co-glycolide) microspheres stabilizes camptothecins, Pharm. Res. 16 (1999) 241–248.

[14] W. Tong, L. Wang, M.J. D'Souza, Evaluation of PLGA microspheres as delivery system for antitumor agent-camptothecin, Drug Dev. Ind. Pharm. 29 (2003) 745–756.

[15] G.T. Colbern, D.J. Dykes, C. Engbers, R. Mumeter, A. Hiller, E. Pegg, R. Saville, S. Wenig, M. Luzzio, P. Uster, M. Amantea, P.K. Working, Encapsulation of the topoisomerase I inhibitor GI147211C in pegylated (STEALTH) liposomes: pharmacokinetics and antitumor activity in HT29 colon tumor xenografts, Clin. Cancer Res. 4 (1998) 3077–3082.

[16] C.L. Messerer, E.C. Ramsay, D. Waterhouse, R. Ng, E.M. Simms, N. Hanaym, P. Tardi, L.D. Mayer, M.B. Bally, Liposomal irinotecan: formulation development and therapeutic assessment in murine xenograft models of colorectal cancer, Clin. Cancer Res. 10 (2004) 6638–6649.

[17] A. Tanizawa, A. Fujimori, Y. Fujimori, Y. Pommier, Comparison of topoisomerase I inhibition, DNA damage, and cytotoxicity of camptothecin derivatives presently in clinical trials, J. Natl. Cancer Inst. 86 (1994) 836–842.

[18] M. Yokoyama, P. Opanasopit, T. Okano, K. Kawano, Y. Maitani, Polymer design and incorporation methods for polymeric micelle carrier system containing water insoluble anti-cancer agent camptothecin, J. Drug Target. 12 (2004) 373–384.

[19] P. Opanasopit, M. Yokoyama, M. Watanabe, K. Kawano, Y. Maitani, T. Okano, Block copolymer design for camptothecin incorporation into polymeric micelles for passive tumor targeting, Pharm. Res. 21 (2004) 2001–2008.

[20] Y. Matsumura, H. Maeda, A new concept for macromolecular therapeutics in cancer chemotherapy: mechanism of tumoritropic accumulation of proteins and the antitumor agent smancs, Cancer Res. 46 (1986) 6387–6392.

[21] H. Maeda, The enhanced permeability and retention (EPR) effect in tumor vasculature, The key role of tumor-selective macromolecular drug targeting, Adv. Enzyme Regul. 41 (2000) 189–207.

[22] H. Maeda, J. Wu, T. Sawa, Y. Matsumura, K. Hori, Tumor vascular permeability and the EPR effect in macromolecular therapeutics: a review, J. Control. Release 65 (2000) 271–284.

[23] K. Ogawara, K. Furumoto, S. Nagayama, K. Minato, K. Higaki, T. Kai, T. Kimura, Pre-coating with serum albumin reduces receptor-mediated hepatic disposition of polystyrene nanosphere: implications for rational design of nanoparticles, J. Control. Release 100 (2004) 451–455.

[24] V.S.K. Balagurusamy, G. Ungar, V. Percec, G. Johansson, Rational design of the first spherical supramolecular dendrimers self-organized in a novel thermotropic cubic liquid-crystalline phase and the determination of their shape by X-ray analysis, Am. Chem. Soc. 119 (1997) 1539–1555.

[25] S.C. Yang, L.F. Lu, Y. Cai, J.B. Zhu, B.W. Liang, C.Z. Yang, Body distribution in mice of intravenously injected camptothecin solid lipid nanoparticles and targeting effect on brain, J. Control. Release 59 (1999) 299–307.

[26] D.L. Warner, T.G. Burke, Simple and versatile high-performance liquid chromatographic method for the simultaneous quantitation of the lactone and carboxylate forms of camptothecin anticancer drugs, J. Chromatogr. B Biomed. Sci. Appl. 691 (1997) 161–171.

[27] H. Onishi, Y. Machida, Y. Machida, Antitumor properties of irinotecan-containing nanoparticles prepared using poly(DL-lactic acid) and poly (ethylene glycol)-block-poly(propylene glycol)-block-poly(ethylene glycol), Biol. Pharm. Bull. 26 (2003) 116–119.

[28] S. Takemoto, K. Yamaoka, M. Nishikawa, Y. Tabata, m, Histogram analysis of pharmacokinetic parameters by bootstrap resampling from one-point sampling data in animal experiments, Drug Metab. Pharmacokinet. 21 (2006) 458–464.

[29] R.P. Hertzberg, M.J. Caranfa, K.G. Holden, D.R. Jakas, G. Gallagher, M.R. Mattern, S.M. Mong, J.O. Bartus, R.K. Johnson, W.D. Kingsbury, Modification of the hydroxy lactone ring of camptothecin: inhibition of mammalian topoisomerase I and biological activity, J. Med. Chem. 32 (1989) 715–720.

[30] V.P. Torchilin, V.R. Rerdichevsky, A.A. Bazukov, V.N. Smirnov, Coating liposomes with protein decreases their capture by macrophages, FERS Lett. 111 (1980) 184–188.

[31] Y. Zou, Q.P. Wu, W. Tansey, D. Chow, M.C. Hung, C. Charnsangavej, S. Wallace, C. Li, Effectiveness of water soluble poly(L-glutamic acid)-camptothecin conjugate against resistant human lung cancer xenografted in nude mice, Int. J. Oncol. 18 (2001) 331–336.

[32] M. Zamai, M. VandeVen, M. Farao, E. Gratton, A. Ghiglieri, M.G. Castelli, E. Fontana, R. D'Argy, A. Fiorino, E. Perenti, A. Suarato, V.R. Caiolfa, Camptothecin poly[n-(2-hydroxypropyl) methacrylamide] copolymers in antitopoisomerase-I tumor therapy: intratumor release and antitumor efficacy, Mol. Cancer Ther. 2 (2003) 29–40.

[33] Y. Maitani, S. Katayama, K. Kawano, A. Hayama, K. Yoma, Artificial lipids stabilized camptothecin incorporated into liposomes, Biol. Pharm. Bull. (in press).

Journal of Controlled Release 129 (2008) 124–127

Contents lists available at ScienceDirect

Journal of Controlled Release

journal homepage: www.elsevier.com/locate/jconrel

High gene delivery in tumor by intratumoral injection of tetraarginine-PEG lipid-coated protamine/DNA

Takashi Fujita [a], Masahiko Furuhata [a], Yoshiyuki Hattori [a], Hiroko Kawakami [b], Kazunori Toma [b], Yoshie Maitani [a,*]

[a] Institute of Medicinal Chemistry, Hoshi University, Ebara 2-4-41, Shinagawa-ku, Tokyo 142-8501, Japan
[b] The Noguchi Institute, Kaga 1-8-1, Itabashi-ku, Tokyo 173-0003, Japan

ARTICLE INFO

Article history:
Received 4 March 2008
Accepted 16 April 2008
Available online 23 April 2008

Keywords:
Oligoarginine
Protamine
DNA delivery
Intratumor injection
In vivo transfection

ABSTRACT

One obstacle to effective gene therapy lies in low transfection efficiency by non-viral vectors. To meet this challenge, we developed cell-penetrating peptide-based gene delivery vectors. A novel oligoarginine lipid ((Arg)n-8, n=4, 10) conjugated to 3,5-bis(dodecyloxy)benzamide (BDB) lipid with a poly(ethylene glycol) (PEG) spacer was synthesized. Oligoarginine lipid-coated vector was prepared by the addition of (Arg)n-8 to DNA/protamine complex (PD) ((Arg)n-8-PD). Transfection efficiency of (Arg)n-8-PD was compared with that of (Arg)n-8/DNA complex ((Arg)n-8/D) for in vitro and in xenograft tumor of human cervical carcinoma HeLa by intratumoral injection. Transfection efficiency in tumors and in vitro greatly depended on the charge ratios of (Arg)n-8 to DNA and the length of Arg residues. In vitro, positively charged Arg10-8-PD showed the highest transfection efficiency. In contrast, in tumor transfection, negatively charged Arg4-8-PD showed the highest transfection efficiency, about 2-, 16- and 23-fold higher than PD alone, Arg10-8-PD and a commercial gene transfection reagent, respectively. This result suggests that negatively charged tetraarginine-conjugated-PEG lipid-coated PD is a promising gene delivery vector for intratumoral injection.

1. Introduction

One obstacle to effective gene therapy lies in low transfection efficiency using non-viral vectors. To overcome these problems, oligoarginine which is one of cell-penetrating peptides (CPPs) such as HIV-1 Tat fragments, has attracted much attention because CPPs can deliver their associated molecules into cells via a unique mechanism [1–6]. Since oligoarginine has similar characteristic to CPPs, it has been used to deliver its associated molecules; genes and proteins into cells [5,7–9]. In an in vitro experiment, oligoarginine, consisting of 8 residues, showed high transfection efficiency [7]. In an in vivo experiment, octaarginine-linked stearyl residue by intravenous injection showed high transfection efficiency [10].

Many research papers including ours reported that the optimal charge ratios of cationic liposomes to DNA of lipoplexes for gene transfection were different between in vitro and in vivo [11]. Accordingly, there is a possibility that optimal oligoarginine length is different in vitro and in vivo, corresponding to charge ratios. To the best of our knowledge, however, there is no report on the effect of oligoarginine length against transfection efficiency of intratumoral injection using oligoarginine vectors. We previously reported a novel gene vector ((Arg)n-8) which composed of oligoarginine ((Arg)n; n=4, 6, 8, 10) conjugated 3,5-bis(dodecyloxy)benzamide (BDB) lipid with a poly(ethylene glycol) (PEG) spacer. Arg10-8 complexed with plasmid DNA (DNA) (Arg10-8/D) has the highest transfection efficiency among the (Arg)n-8 in vitro [12]. We also found that Arg4-modified liposome alone showed the highest cellular uptake regardless of the lowest transfection efficiency, and was able to deliver associated smaller protein efficiently among (Arg)n-8 [13].

Here to develop an in vivo transfection vector, we focused on Arg4-8 with high gene delivery ability by improvement of release DNA in cytoplasm. Protamine could enhance lipid-mediated gene transfer better than poly-L-lysine [14]. We therefore changed the vector formation from (Arg)n-8/D to (Arg)n-8-coated DNA complexes with protamine (PD) (Arg)n-8-PD) to enable DNA to be released easily, and compared transfection efficiency at various charge ratios (+/−) of (Arg)n-8 to DNA in vitro and in an xenograft tumor of human cervical carcinoma HeLa by intratumoral injection.

2. Materials and methods

(Arg)n-8 (Fig. 1) was synthesized as previously reported [12]. Protamine sulfate (grade III) was purchased from Sigma-Aldrich (St. Louis, MO). The Pica gene luciferase assay kit was purchased from Toyo Ink (Tokyo, Japan). Fetal bovine serum (FBS), L-glutamine, Earle's minimum essential medium (EMEM) and Lipofectamine™ 2000 (LA2000) were purchased from Invitrogen Corp. (Carlsbad, CA). Non-

* Corresponding author. Tel./fax: +81 3 5498 5048.
E-mail address: yoshie@hoshi.ac.jp (Y. Maitani).

0168-3659/$ – see front matter © 2008 Elsevier B.V. All rights reserved.
doi:10.1016/j.jconrel.2008.04.010

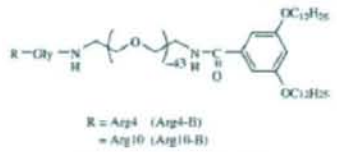

R = Arg4 (Arg4-B)
= Arg10 (Arg10-B)

Fig. 1. Chemical structure of (Arg)n-B.

essential amino acids (NEAA) were purchased from Dainippon Pharmaceutical Corp., Ltd (Osaka, Japan). In vivo-jetPEI™ (PEI) was purchased from Polyplus-transfection (Ulkirch, France). All other chemicals were of reagent grade. The plasmid pCMV-luc encoding the luciferase gene under the control of the CMV promoter and the plasmid pEGFP-C1 encoding enhanced green fluorescent protein (EGFP) under the CMV promoter were described in previous reports [12,15]. HeLa cells were purchased from ECACC (Wiltshire, U.K.), and grown in EMEM supplemented with 2 mM L-glutamine, 1% NEAA and 10% FBS at 37 °C in a humidified 5% CO_2 atmosphere.

To form (Arg)n-B/D, (Arg)n-B aqueous solution was added to an aqueous solution of DNA at charge ratios (+/−) of (Arg)n-B to DNA of 0.01–1.0. One molecule of Arg4- and Arg10-B was considered (+1) charge, not depending on the number of arginine residues. To form PD, an aqueous solution of protamine was added to the DNA aqueous solution with rapid vortexing to achieve (+/−) of protamine to DNA of 0.001–0.5 (PD(0.001–0.5)). In a preliminary experiment, Arg4-B-PD at a charge ratio (+/−) of Arg4-B to DNA of 1.0, PD(0.3) showed higher luciferase activity than at PD(0.1), and similar activity to at PD(0.5) (Supplement Fig. S1). The formulation of (Arg)n-B-PD(0.3) therefore was selected in the subsequent experiment. To form (Arg)n-B-PD(0.3), (Arg)n-B aqueous solution was added of to anionic PD(0.3) suspension, and adjusted at charge ratios (+/−) of (Arg)n-B to DNA of 0.01–1.0.

Each complex was left at room temperature for 10–15 min before transfection. Particle size and zeta potential of PD and (Arg)n-B vectors were measured using ELS-Z2 (Otsuka Electronics Co. Ltd, Osaka, Japan) as already reported [12,13]. In a preliminary experiment, Arg4-B-PD at a charge ratio (+/−) of Arg4-B to DNA of 1.0, PD at a charge ratio (+/−) of 0.3 (PD(0.3)) showed higher luciferase activity than at PD(0.1), and similar activity to at PD(0.5) (Supplement Fig. S1); therefore, the formulation of (Arg)n-B-PD(0.3) was selected in the subsequent experiment.

In vitro gene transfection and luciferase assay were described in a previous report [12]. For in vivo gene transfection, female BALB/cAJcl-nu/nu mice (6 weeks old) were obtained from CLEA Inc. (Tokyo, Japan). To generate HeLa tumor xenografts, 2.1×10^7 cells were inoculated subcutaneously into the flank region of the mice. A total of 40 μL of each particle complex and DNA aqueous solution was injected intratumorally at a dose of 10 μg DNA per tumor. For transfection with PEI, 1.2 μL of PEI solution was used for 10 μg of DNA to form a DNA complex at a charge ratio (+/−) of 6 in 40 μL of 5% glucose, according to the manufacturer's protocol. Tumor was collected and homogenized with luciferase cell culture lysis reagents (Promega Co., Madison, WI). The tumor supernatants were frozen at −80 °C and thawing at 37 °C, followed by centrifugation. Luciferase assay was described in a previous report [12]. For in vivo GFP expression, the frozen organs were sliced into 10 μm sections and GFP expression in tumors was observed by fluorescence microscopy (ECLIPSE TS100-F, Nikon, Tokyo, Japan).

Significant differences in the mean values were evaluated by Student's unpaired *t*-test and one-way ANOVA followed by post-hoc analysis using Dunnett's test. A *p*-value of less than 0.05 was considered significant.

3. Results and discussion

Particle size and zeta potential of vectors are major parameters governing gene transfection activity. Particle sizes of PD(0.1–0.5), (Arg)n-B/D and (Arg)n-B-PD(0.3) were about 100 nm, 150–220 nm, and 150–180 nm, respectively (Fig. 2). The particle sizes of (Arg)n-B/D at a charge ratio (+/−) of 0.01 could not be measured due to the low concentration of lipid. The zeta potentials of DNA and PD were about −60 mV and −30 mV, respectively. The zeta potential of (Arg)n-B/D and (Arg)n-B-PD(0.3) increased in parallel with the increasing charge ratio (+/−) of (Arg)n-B to DNA. (Arg)n-B/D exhibited a positive charge at a charge ratio

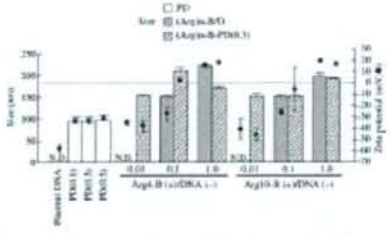

Fig. 2. Size and zeta potential of PD and (Arg)n-B vectors as a function of the charge ratio (+/−) of protamine, Arg4-B, or Arg10-B to DNA. Charge ratio (+/−) of PD in (Arg)n-B-PD was 0.3. Each bar represents the mean ± S.D. of three experiments. N.D., not detected.

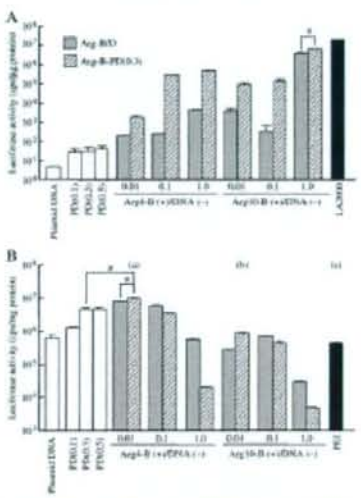

Fig. 3. Effect of charge ratio (+/−) of protamine to DNA for PD or (Arg)n-B to DNA for vectors on luciferase activity in HeLa cells (A) and in tumors (B). Charge ratio (+/−) of PD in (Arg)n-B-PD was 0.3. (A) After incubation for 3 h in serum-free EMEM, cells were further incubated for 21 h at 37 °C in EMEM containing 10% FBS. (B) Luciferase activity in tumor 24 h after intratumoral injection of vector/DNA complex into mice at a dose of 10 μg DNA per tumor. Each bar represents the mean ± S.D. of three experiments. Asterisk: $P<0.05$.

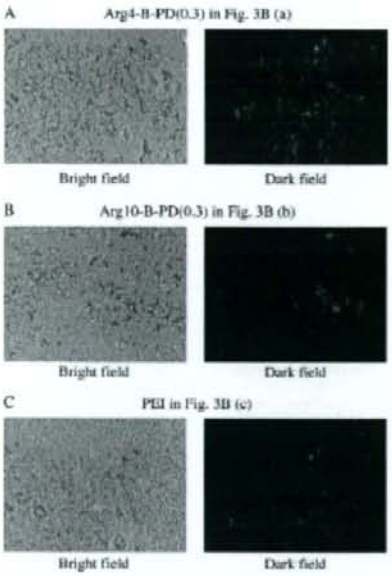

Fig. 4. Analysis of GFP expression in HeLa tumor by fluorescence microscope 24 h after intratumoral injection into BALB/cAJcl-nu/nu mice using (Arg)n-B-PD(0.3); Arg4-B-PD (0.3) (A) and Arg10-B-PD(0.3) (B) and PEI (C), corresponding to (a), (b) and (c) in Fig. 3B, respectively. Magnification ×100.

of 1.0, but (Arg)n-B-PD(0.3) became nearly positive at a charge ratio of 0.1, because (Arg)n-B-PD(0.3) contained protamine. (Arg)n-B is water-soluble and, hence, may coat PD(0.3). It was confirmed that the zeta potential of (Arg)n-B-PD(0.3) was changed from negatively charged PD (0.3) alone (−30 mV) to a decreased negative charge or positive charge with the increase of (Arg)n-B.

First, we evaluated the transfection efficiency of the vectors and naked DNA by assaying luciferase activity in HeLa cells (Fig. 3A) and in the xenograft tumor after intratumoral injection (Fig. 3B). PD(0.1–0.5) increased luciferase activity compared with naked DNA. Transfection efficiency increased with an increase of the charge ratio (+/−) of (Arg)n-B/D and (Arg)n-B-PD(0.3) where all (Arg)n-B-PD(0.3) showed higher transfection efficiency than the corresponding (Arg)n-B/D. Arg4- and Arg10-B-PD(0.3) at a charge ratio (+/−) of 1.0 increased luciferase activity about 140- and 2-fold compared with Arg4- and Arg10-B/D, respectively, where Arg10-B-PD(0.3) was the highest among vectors, showing about 3-fold-lower transfection efficiency than a commercial gene transfection reagent, LA2000.

Protamine is a cationic peptide consisting of arginine residues and has been reported to act as a nuclear localization signal [16–18] and has a possibility to facilitate the intracellular release of nucleic acid [19]. Accordingly, DNA partially neutralized with protamine may promote the release of DNA from endosome to the cytoplasm and the penetration of DNA into the nucleus. Flow cytometric analysis showed that cellular uptake of Arg4-B-PD(0.3) in the cells was almost the same as Arg10-B-PD(0.3) when using FITC-ODN (Supplement Fig. S2). These results suggested that Arg10-B and Arg4-B had similar gene delivery ability into the cells, and the former could release the gene into the nucleus but the latter could not, likely due to strong binding with DNA without neutralization by protamine.

The in vivo transfection experiment showed an inverse correlation with the in vitro experiment. Arg4-B-PD(0.3) at a charge ratio (+/−) of 0.01 had the highest transfection efficiency among the vectors, about 2-, 16- and 23-fold compared with PD(0.3), Arg10-B-PD(0.3) at a charge ratio (+/−) of 0.01 and a commercial gene transfection reagent, PEI, respectively (Fig. 3B). These results indicated that the in vitro system for evaluating oligoarginine-mediated gene delivery did not reflect the optimal condition of in vivo gene delivery.

To confirm gene expression in the tumor, we observed the gene expression of the plasmid pEGFP-C1 with (Arg)n-B-PD(0.3) using fluorescence microscopy (Fig. 4). GFP expression was observed for Arg4-B-PD(0.3) in a wider region than for Arg10-B-PD(0.3) at a charge ratio (+/−) of 0.01 and PEI, corresponding with the result of luciferase expression in the tumor (Fig. 3B, (a),(b),(c)), and suggesting that cationic particles could not spread widely in tissue after intratumoral injection.

Although Arg4- and Arg10-B-PD(0.3) at a charge ratio (+/−) of 1.0 had 5 μM (Arg)n-B concentration, and similar particle size and zeta potentials, their transfection efficiencies were quite different in the tumor, suggesting that oligoarginine length was an important factor for intratumoral gene delivery. Protamine properly neutralized the charge of DNA. Arg4-B therefore may interact with cells as CPP, and spread widely in tumors. Although the longer oligoarginine of Arg10-B showed high transfection efficiency in vitro, in which the positive charge of Arg10-B was partially used for translocation through the plasma membrane and for the formation of complex with DNA, excess arginine residues of Arg10-B might inhibit the spread of Arg10-B-PD (0.3) by interaction with tissue proteins. This finding corresponded to the result when direct injection of naked DNA into solid tumor resulted in a high level of transfection, but cationic lipid-based vector inhibited gene expression [20–22]. The difference in gene expression between in vitro and in vivo might be due to the difference of accumulation vector/DNA complexes near tumor cells. Arg4-B-PD(0.3) at a charge ratio (+/−) of 0.01 exhibited significantly higher transfection efficiency than similar negatively charged PD(0.3), indicating that Arg4-B probably coated on PD(0.3) worked effectively for intratumoral gene delivery.

Acknowledgements

This project was supported in part by a grant from the Promotion and Mutual Aid Corporation for Private Schools of Japan and by a Grant-in-Aid for Scientific Research from the Ministry of Education, Culture, Sports, Science, and Technology of Japan and by the Open Research Center Project.

Appendix A. Supplementary data

Supplementary data associated with this article can be found, in the online version, at doi:10.1016/j.jconrel.2008.04.010.

References

[1] D. Derossi, A.H. Joliot, G. Chassaing, A. Prochiantz, The third helix of the Antennapedia homeodomain translocates through biological membranes, J. Biol. Chem. 269 (1994) 10444–10450.

[2] J. Oehlke, A. Scheller, B. Wiesner, E. Krause, M. Beyermann, E. Klaudtner, M. Melzig, M. Bienert, Cellular uptake of an alpha-helical amphipathic model peptide with the potential to deliver polar compounds into the cell interior non-endocytically, Biochim. Biophys. Acta 1414 (1998) 127–139.

[3] M. Pooga, M. Hallbrink, M. Zorko, U. Langel, Cell penetration by transportan, FASEB J. 12 (1998) 67–77.

[4] E. Vives, P. Brodin, B. Lebleu, A truncated HIV-1 Tat protein basic domain rapidly translocates through the plasma membrane and accumulates in the cell nucleus, J. Biol. Chem. 272 (1997) 16010–16017.

[5] S. Futaki, T. Suzuki, W. Ohashi, T. Yagami, S. Tanaka, K. Ueda, Y. Sugiura, Arginine-rich peptides. An abundant source of membrane-permeable peptides having potential as carriers for intracellular protein delivery, J. Biol. Chem. 276 (2001) 5836–5840.
[6] M.C. Morris, J. Depollier, J. Mery, F. Heitz, G. Divita, A peptide carrier for the delivery of biologically active proteins into mammalian cells, Nat. Biotechnol. 19 (2001) 1173–1176.
[7] S. Futaki, W. Ohashi, T. Suzuki, M. Niwa, S. Tanaka, K. Ueda, H. Harashima, Y. Sugiura, Stearylated arginine-rich peptides: a new class of transfection systems, Bioconjug. Chem. 12 (2001) 1005–1011.
[8] D.J. Mitchell, D.T. Kim, L. Steinman, C.G. Fathman, J.B. Rothbard, Polyarginine enters cells more efficiently than other polycationic homopolymers, J. Pept. Res. 56 (2000) 318–325.
[9] P.A. Wender, D.J. Mitchell, K. Pattabiraman, E.T. Pelkey, L. Steinman, J.B. Rothbard, The design, synthesis, and evaluation of molecules that enable or enhance cellular uptake: peptoid molecular transporters, Proc. Natl. Acad. Sci. U. S. A. 97 (2000) 13003–13008.
[10] H. Hatakeyama, H. Akita, K. Kogure, M. Oishi, Y. Nagasaki, Y. Kihira, M. Ueno, H. Kobayashi, H. Kikuchi, H. Harashima, Development of a novel systemic gene delivery system for cancer therapy with a tumor-specific cleavable PEG-lipid, Gene Ther. 14 (2007) 68–77.
[11] Y. Hattori, W.X. Ding, Y. Maitani, Highly efficient cationic hydroxyethylated cholesterol-based nanoparticle-mediated gene transfer in vivo and in vitro in prostate carcinoma PC-3 cells, J. Control. Release 120 (2007) 122–130.
[12] M. Furutsu, H. Kawakami, K. Toma, Y. Hattori, Y. Maitani, Design, synthesis and gene delivery efficiency of novel oligo-arginine-linked PEG lipids: effect of oligo-arginine length, Int. J. Pharm. 316 (2006) 105–116.
[13] M. Furutsu, H. Kawakami, K. Toma, Y. Hattori, Y. Maitani, Intracellular delivery of proteins in complexes with oligoarginine-modified liposomes and the effect of oligoarginine length, Bioconjug. Chem. 17 (2006) 1035–1042.
[14] P.L. Sorgi, S. Bhattacharya, L. Huang, Protamine sulfate enhances lipid-mediated gene transfer, Gene Ther. 4 (1997) 961–968.
[15] S. Igarashi, Y. Hattori, Y. Maitani, Biosurfactant MEL-A enhances cellular association and gene transfection by cationic liposome, J. Control. Release 112 (2006) 362–368.
[16] Y.H. Ni, M.Y. Hsu, P.J. Chen, M.H. Chang, Protamine enhances the efficiency of liposome-mediated gene transfer in a cultured human hepatoma cell line, J. Formos. Med. Assoc. 98 (1999) 562–566.
[17] D.P. Yang-Lee-ard, S.J. Han, L. Huang, Lipid–protamine-DNA-mediated antigen delivery, Curr. Drug Deliv. 2 (2005) 401–406.
[18] A. Noguchi, N. Hirashima, M. Nakanishi, Cationic cholesterol promotes gene transfection using the nuclear localization signal in protamine, Pharm. Res. 19 (2002) 918–924.
[19] M.L. Read, K.H. Bremner, D. Oupicky, N.K. Green, P.F. Searle, L.W. Seymour, Vectors based on reducible polycations facilitate intracellular release of nucleic acids, J. Gene Med. 5 (2003) 232–245.
[20] J.P. Yang, L. Huang, Direct gene transfer to mouse melanoma by intratumor injection of free DNA, Gene Ther. 3 (1996) 542–548.
[21] T. Nomura, K. Yasuda, T. Yamada, S. Okamoto, K.I. Mahato, Y. Watanabe, Y. Takakura, M. Hashida, Gene expression and anti-tumor effects following direct interferon (IFN)-gamma gene transfer with naked plasmid DNA and DC-chol liposome complexes in mice, Gene Ther. 6 (1999) 121–129.
[22] P. Reyrat, D. Rhane, A. Cao, N. Lievre, R. Naejus, P. Rainteau, J.L. Salmmann, F. Tailandier, In vitro and in vivo transfection of melanoma cells B16-F10 mediated by cholesterol-based cationic liposomes, J. Drug Target. 10 (2002) 557–566.

European Journal of Pharmaceutics and Biopharmaceutics 70 (2008) 718–725

Contents lists available at ScienceDirect

European Journal of Pharmaceutics and Biopharmaceutics

journal homepage: www.elsevier.com/locate/ejpb

Research paper

Folate-linked lipid-based nanoparticles for synthetic siRNA delivery in KB tumor xenografts

Takashi Yoshizawa, Yoshiyuki Hattori *, Motoki Hakoshima, Kimiko Koga, Yoshie Maitani

Institute of Medicinal Chemistry, Hoshi University, Tokyo, Japan

ARTICLE INFO

Article history:
Received 18 September 2007
Accepted in revised form 20 June 2008
Available online 4 July 2008

Keywords:
Folic acid
Folate receptor
Synthetic siRNA
Cationic nanoparticles
Nasopharyngeal tumor
Her-2

ABSTRACT

RNA interference (RNAi) is a sequence-specific gene-silencing mechanism triggered by synthetic small interfering RNA (siRNA), and is utilized in a wide range of fields including cancer gene therapy by down-regulating a specific target protein. In this study, for tumor-targeted siRNA delivery, we developed a folate-linked nanoparticle (NP-F), and evaluated the potential of NP-F-mediated tumor gene therapy in human nasopharyngeal KB cells, which overexpressed folate receptor (FR). NP-F was composed of cholesteryl-3β-carboxyamidoethylene-*N*-hydroxyethylamine (OH-Chol), Tween 80 and folate-poly(ethylene glycol)-distearoylphosphatidylethanolamine conjugate (f-PEG$_{2000}$-DSPE), and NP-P was substituted f-PEG$_{2000}$-DSPE in NP-F PEG$_{2000}$-DSPE for a non-targeting nanoparticle. The NP-F and siRNA complex (nanoplex) formed at a charge ratio (+/−) of 2/1 in the presence of 5 mM NaCl was injectable size and increased transfection efficiency in the cells. NP-F showed a significantly higher intracellular amount of siRNA and stronger localization of siRNA in the cytoplasm than NP-P. When Her-2 siRNA was transfected into cells by NP-F and NP-P, NP-F significantly inhibited tumor growth, and selectively suppressed Her-2 protein expression more than NP-P. In in vivo gene therapy, a NP-F nanoplex of Her-2 siRNA by intratumoral injection significantly inhibited tumor growth of KB xenografts compared with control siRNA, but a NP-P nanoplex did not. These results of the experiments have provided optimal conditions to form folate-linked nanoparticle complexes with siRNA for folate-targeted gene therapy.

1. Introduction

RNA interference (RNAi) is a post-transcriptional mechanism of gene silencing mediated by cleavage of target RNA [1]. This phenomenon occurs by small interfering RNA (siRNA) in the cytoplasm of mammalian cells [2]. In siRNA technology, two delivery mechanisms were considered; direct delivery of synthetic siRNA nucleotide, and introduction of a plasmid DNA (pDNA) encoding a short hairpin construct (shRNA) that will be enzymatically degraded into siRNA. Synthetic siRNAs, which are 21–28 bp small double-stranded RNA, are substrates for the RNA-induced silencing complex. RNAi has potential not only as a tool in biological analysis but also as an evolutional drug for cancer and other diseases. To elevate their gene inhibition effect, many vectors were used to attempt to deliver synthetic siRNA and pDNA encoding as shRNA [3].

Viral vectors like retrovirus- [4,5], adenovirus- [6–8] and lentivirus-based vectors [9–11] have been successful in obtaining efficient and long gene silencing using siRNA. Among them, adenoviral vectors are widely used both *in vitro* and *in vivo*, however; they possess high immunogenicity and proinflammatory effects. Hydrodynamic injections of naked synthetic siRNA have led to the silencing of endogenous genes in various animal tissues, which include the liver, spleen, lung, kidney and pancreas [12–14]. However, the need for a large volume limits this method of delivery *in vivo*. Alternative delivery technologies such as formulated synthetic siRNA using liposomes or atelocollagen as carriers have been reported [3,15,16]. Cationic liposomes are routinely used for gene delivery of pDNA and have recently been applied for synthetic siRNA delivery [17]; therefore, reports of synthetic siRNA delivery strategies are very limited compared with pDNA delivery.

Cancer therapy with synthetic siRNA or pDNA encoding shRNA needs a selective delivery system to the tumor. The receptor for folic acid has been identified as a marker for ovarian carcinomas [18] and has also been found to be frequently overexpressed in a wide range of tumors [18,19]; therefore, folic acid was utilized as tumor-targeting ligand for the delivery of chemotherapeutic agents, pDNA, and antisense ODN to receptor-bearing tumor cells [20–23]. However, there has been no report about folate receptor (FR)-targeting delivery of synthetic siRNA and pDNA encoding shRNA except for cationic polymer folate-PEG-PEI [24,25]. Folate-PEG-PEI of EGFP siRNA exhibited effective suppression of EFGP into EGFP stably expressed human nasopharyngeal tumor KB cells compared with PEI, however; it has not been applied for cancer therapy with antitumor siRNA.

* Corresponding author. Institute of Medicinal Chemistry, Hoshi University, Ebara 2-4-41, Shinagawa-ku, Tokyo 142-8501, Japan. Tel./Fax: +81 3 5498 5097.
E-mail address: yhattori@hoshi.ac.jp (Y. Hattori).

0939-6411/$ - see front matter © 2008 Elsevier B.V. All rights reserved.
doi:10.1016/j.ejpb.2008.06.026

Recently, we demonstrated that folate-linked nanoparticles (NP-F) greatly increased transfection efficiency when the NP-F nanoplex of pDNA was formed in the presence of NaCl [26]. In this study, we evaluated the potential of NP-F to deliver synthetic siRNAs to tumor *via* FR and the therapeutic effect of siRNA targeted for Her-2 protein in KB tumor cells and xenografts.

2. Materials and methods

2.1. Materials

Cholesteryl-3β-carboxyamide ethylene-*N*-hydroxyethylamine (OH-Chol) was synthesized as previously described [26]. Poly(ethylene glycol)-distearoylphosphatidylethanolamine (PEG_{2000}-DSPE) and Tween 80 were obtained from NOF Co. (Tokyo, Japan). Folate-polyethyleneglycol-distearoylphosphatidylethanolamine (F-PEG_{2000}-DSPE) (mean MW of PEG: 2 kDa) was synthesized as previously described [27].

2.2. Synthetic siRNA

Duplexed stealth siRNAs targeting against human Her-2 mRNA (Her-2 siRNA), Stealth™ RNAi Negative Control Duplexes Medium GC and Low GC (control-M and control-L siRNAs, respectively) (Invitrogen, Carlsbad, CA, USA) were used for the control of Her-2 siRNA, respectively. The sequences of these siRNAs were as follows: Her-2 sense strand, 5′-AAACGUGUCUGUGUUUCUAGGUGACC-3′; Her-2 antisense strand, 5′-GGUCACCUACAACACAGACACGUUU-3′.

EGFP siRNA, random siRNA, and 5′-carboxyfluorescein (FAM)-labeled GL3 siRNA were purchased from Hokkaido System Science (Hokkaido, Japan). Sequences of GL3 were designed for negative control as previously reported [3]. The sequences of EGFP and random siRNAs were as follows: EGFP siRNA sense strand, 5′-ACGGCAUCAAGGUGAACUUCAAGAUAG-3′ and EGFP siRNA antisense strand, 5′-AUCUUGAAGUUCACCUUGAUGCCGUAU-3′; random siRNA sense strand, 5′-CGAUUCGCUAGACCGGCUUCAUUGCAG-3′ and siRNA antisense strand, 5′-GCAAUGAAGCCGGUCUAGCGAAUCGAU-3′.

2.3. Cell culture

KB cells were supplied by the Cell Resource Center for Biomedical Research, Tohoku University (Miyagi, Japan). The cells were grown in folate-deficient RPMI-1640 medium (Invitrogen, Carlsbad, CA, USA) supplemented with 10% heat-inactivated fetal bovine serum (FBS, Invitrogen) and kanamycin (100 μg/ml) at 37 °C in a 5% CO_2 humidified atmosphere.

2.4. Preparation of nanoparticles and nanoplexes

Nanoparticles were prepared by a modified ethanol injection method as previously described [26]. Briefly, the formulation of nanoparticle consisted of 1 mg/ml OH-Chol as a cationic lipid, and 5 mol% Tween 80 (NP). NP-F and NP-P were incorporated with 1 mol% f-PEG_{2000}-DSPE or 1 mol% PEG_{2000}-DSPE into the NP formulation. For example, in the case of NP-F, OH-Chol:Tween 80:f-PEG_{2000}-DSPE = 94:5:1 molar ratio (≈10:1.3:0.65, weight) was dissolved in about 5 ml of ethanol, then the ethanol was removed with a rotary evaporator until 1–2 ml was left. Next, a constant volume of water was added to the ethanol solution. Nanoparticles formed instantly after further evaporation of the residual ethanol. The concentration of OH-Chol was adjusted to 1 mg/ml in the final nanoparticle suspension with a drop of water. Then the nanoparticle suspension was filtered through 0.45 μm Millex-HA filters (Millipore, Cork, Ireland) to sterilize it. In 1,1′-dioctadecyl-3,3,3′,3′-tetramethylindocarbocyanine perchlorate (DiI) (Lambda Probes & Diagnostics, Graz, Austria)-labeled nanoparticles, DiI was incorporated at 0.04 mol% of total lipid.

To prepare nanoplexes of siRNA, siRNA was mixed with aliquots of each nanoparticle in water, 5 or 10 mM NaCl solution, and the mixture was kept at room temperature for 15 min. Particle size distributions and ζ-potentials were measured by ELS-Z2 (Otsuka Electronics Co., Osaka, Japan) at 25 °C after diluting the dispersion to an appropriate volume with water.

2.5. Gel retardation assay

One microgram of pDNA, double-stranded oligodeoxynucleotide (dsODN), and siRNA were mixed with nanoparticles at various charge ratios (+/−) from 1/1 to 4/1 in water. After 15 min incubation of the nanoplexes, they were analyzed by 1.5% agarose gel for pDNA or 12.5% acrylamide gel electrophoresis for siRNA and dsODN in Tris–Borate–EDTA (pH 8.0, TBE) buffer and detected by ethidium bromide staining as previously reported [26].

2.6. Transfection of siRNA nanoplex

KB cells were prepared by plating cells in a 35 mm culture dish 24 h prior to each experiment. The cells at confluences of 50% in the well were transfected with each nanoplex. Nanoplex at a charge ratio (+/−) of 2/1 or 3/1 was formed by mixing each nanoparticle and siRNA in water or in 5 mM NaCl solution and leaving at room temperature for 15 min. For transfection with lipofectamine 2000, lipofectamine 2000 lipoplex was prepared according to the manufacturer's protocol. Briefly, 5 μl of lipofectamine 2000 was diluted with 125 μl Opti-MEM I® reduced serum medium (Invitrogen) and incubated for 5 min. The mixture was combined with 100 pmol siRNA diluted with 125 μl Opti-MEM I® reduced serum medium and then leaving at room temperature for 20 min. The nanoplex and lipoplex were diluted with culture medium containing 10% FBS and incubated with the cells at a final concentration of 100 nM siRNA in the medium for 24 or 48 h at 37 °C.

2.7. Antiproliferative activity

KB cells were seeded in 96-well plates 24 h prior to transfection. Cells at confluences of 50% in the well were transfected with each nanoplex of Her-2 siRNA. We used EGFP, control-M and control-L siRNAs as control siRNAs. Nanoplex at a charge ratio (+/−) of 2/1 or 3/1 was formed in 5 mM NaCl solution, transfected into the cells, and incubated for 72 h. Then, cell viability was measured by WST-8 assay (Dojindo Laboratories, Kumamoto, Japan).

2.8. Western blot analysis

Cells were seeded in a 35 mm culture dish 24 h before transfection. Nanoplex of Her-2, EGFP and control-M siRNAs at a charge ratio (+/−) of 2/1 was formed in 5 mM NaCl solution. For transfection with lipofectamine 2000, lipofectamine 2000 lipoplex was prepared according to the manufacturer's protocol. After transfection of the nanoplex, cells were washed in PBS twice. Cell protein extracts were prepared with sampling buffer containing 1% Triton X-100, protease inhibitor cocktail set III (Calbiochem, Darmstadt, Germany) in PBS. After they were centrifuged at 10,000*g* for 10 min, the protein concentration of the supernatant was quantitated with the bicinchoninic acid protein assay reagent (Pierce, Rockford, IL, USA). For the detection of β-actin protein, 5 μg of protein was separated by 12.5% SDS–PAGE, and for the detection of Her-2 protein, 20 μg of protein was separated by 7.5% SDS–PAGE. Then they were transferred to a polyvinylidene difluoride (PVDF) membrane (FluoroTrans® W, PALL Gelman Laboratory, Ann Arbor,

MI, USA). Membranes were blocked in PBS containing 0.1% Tween-20 with 0.5% skimmed milk at 4 °C for 18 h. The blot of Her-2 protein was probed with rabbit anti-human Her-2 antibody (Lab Vision, Fremont, CA, USA). Blots of β-actin protein were probed with rabbit anti-β-actin antibody (Lab Vision). Subsequently, the membranes were incubated with a horseradish peroxidase-conjugated secondary antibody (Santa Cruz Biotechnology, Santa Cruz, CA, USA). Immunoblots were detected using a SuperSignal West Pico Chemiluminescent Substrate (Pierce, Rockford, IL, USA).

2.9. Flow cytometry

KB cells were prepared by plating cells in a 35 mm culture dish 24 h prior to each experiment. Cells at confluences of 50% in the well were transfected with each nanoplex of FAM-labeled siRNA. Twenty-four hours after transfection, the cells were detached with 0.05% trypsin and centrifuged at 1500*g*. The supernatant was removed and the cells were resuspended with 0.1% BSA and 1 mM EDTA in PBS. The suspended cells were filtrated with 42 μm nylon mesh and introduced into a FACSCalibur flow cytometer (Becton Dickinson, San Jose, CA, USA) equipped with a 488 nm argon ion laser using CELLQUEST software (PharMingen, USA). Data for 10,000 fluorescent events were obtained by recording forward scatter (FSC), side scatter (SSC), and green (530/30 nm) fluorescence.

2.10. Confocal microscopy

Nanoplex at a charge ratio (+/−) of 2/1 was formed by mixing each nanoparticle and FAM-labeled GL3 siRNA in water or in 5 mM NaCl solution, and incubating with KB cells for 24 h. The cells were washed twice with PBS and fixed with 4% formaldehyde in PBS for 15 min at room temperature. For staining the nucleus, the fixed cells were washed with PBS and incubated with 0.5 mg/ml of RNase in PBS for 20 min at 37 °C. Subsequently, the cells were washed with PBS and incubated with 2.5 mg/ml propidium iodide (PI) for 5 min at room temperature. Each sample was examined whole in a Radiance 2100 confocal laser-scanning microscope (Bio-Rad, CA, USA) as previously described [27].

2.11. Competition analysis by folic acid or folate receptor antibody

KB cell cultures were prepared by plating cells in a 35 mm culture dish 24 h prior to each experiment. Cells were pre-incubated in the presence or absence of 1 mM folic acid or 20 μg/ml monoclonal antibodies to FR α (Mov18/ZEL, Alexis Biochemicals, CA, USA) for 1 h before transfection. DiI-labeled NP-P or NP-F was mixed with 100 pmol siRNA and then diluted to 100 nM siRNA in 1 ml of folate-deficient-RPMI medium containing 10% FBS. Cells were incubated with the nanoplex for 3 h, and then were analyzed using a FACSCalibur flow cytometer as described in the above section. Data for 10,000 fluorescent events were obtained by recording forward scatter (FSC), side scatter (SSC), and red (585/42 nm) fluorescence.

2.12. Assessment of KB tumor growth

Male BALB/c nu/nu mice (5 weeks of age, CLEA Japan, Inc., Tokyo, Japan) were maintained on a folate-deficient rodent diet (Oriental Yeast Co., Ltd., Tokyo, Japan) on arrival and for the duration of the study. To generate KB tumor xenografts, 1×10^7 cells suspended in 50 μl of PBS were inoculated subcutaneously in the flank region of the mice. The tumor volume was calculated using the formula, tumor volume = $0.5 \times a \times b^2$, where *a* and *b* are the larger and smaller diameters, respectively.

When the average volume of the xenograft tumors reached 80 mm^3 (day 0), these mice were divided into two groups: group I, control-M siRNA (10 μg) as a control; group II, Her-2 siRNA (10 μg). Both experimental groups consisted of six tumors. NP-F or NP-P nanoplexes of 10 μg of siRNA per tumor were directly injected into xenografts on days 0, 2 and 4. Tumor volume was measured at days 0, 2, 4, 5, 7, 8, 9 10 and 11. Tumor volume is shown as the mean ± SE. Animal experiments were conducted with ethical approval from our institutional animal care and use committee.

2.13. Statistical analysis

Statistical differences between different groups were analyzed with one-way analysis of variance on ranks with Tukey–Kramer's post-hoc test. A p value of 0.05 or less was considered significant. For the animal study, statistical comparison was performed by Student's *t*-test.

3. Results and discussion

3.1. Gel retardation assay

Three different cationic nanoparticle formulations were prepared, and all formulations consisted of 1 mg/ml OH-Chol as a cationic lipid and 5 mol% Tween 80 (NP). NP-P consisted of NP with 1 mol% PEG_{2000}-DSPE. For FR-targeted vectors, NP-F consisted of NP with 1 mol% f-PEG_{2000}-DSPE. We previously reported that NP-F modified with 1 mol% f-PEG_{2000}-DSPE could efficiently deliver pDNA into KB cells, which overexpressed FR [26]. First, we evaluated the association of NP-F with siRNA, and compared with that with pDNA or dsODN. The association of siRNA with each nanoparticle was monitored by gel retardation electrophoresis (Fig. 1). The migration pattern of siRNA in the nanoplex changed when the siRNA was mixed with nanoparticles in water at charge ratios (+/−) from 1/1 to 4/1. The migration of siRNA in the nanoplex gradually ceased as the charge ratio increased. Beyond charge ratios (+/−) of 3/1 in NP, and of 4/1 in NP-P and NP-F, no migration was observed. This result suggested that the association of siRNA with the nanoparticles was inhibited by the incorporation of f-PEG_{2000}-DSPE or PEG_{2000}-DSPE into nanoparticles. When the nanoplex complexed with dsODN and pDNA, beyond charge ratios (+/−) of 3/1 in NP, NP-P and NP-F, no migration was observed. siRNA might make a weaker association with nanoparticles than pDNA and ODN.

3.2. Antiproliferative activity

Previously, we demonstrated that transfection activity was significantly increased when the nanoplex was formed in the presence of NaCl solution [26]. It was also reported that lipoplexes formed in 5 mM NaCl solution increased transfection efficiency [28,29]. Furthermore, the nanoplexes formed at charge ratios (+/−) above 4/1 exhibited cytotoxicity by increasing the lipid concentration (data not shown). Therefore, to examine the effect of the charge ratio (+/−) on the selectivity of transfection, we transfected the nanoplex formed in 5 mM NaCl solution at charge ratios (+/−) of 2/1 and 3/1, and compared cell viability among the nanoparticles. First, to confirm the effects of Her-2 siRNA transfected into KB cells by nanoparticles, cell viability was measured by WST-8 assay 72 h after incubation. Her-2 proteins are well-known proteins overexpressed in many tumors and are related to apoptosis and cell growth [30]. Commercially available lipofectamine 2000 was used as a control vector for transfection of siRNA. In the transfection of Her-2 siRNA at a charge ratio (+/−) of 2/1, cell viability was 76%, 109% and 71% in cells transfected by NP, NP-P and NP-F, respectively (Fig. 2A), whereas at a charge ratio (+/−) of 3/1, it was 83%, 88% and 80% by NP, NP-P and NP-F, respectively (Fig. 2B). NP-F and NP-P decreased cell viability at charge ratios (+/−)

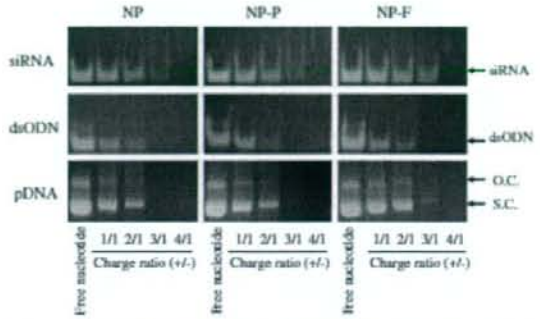

Fig. 1. Association of pDNA, dsODN or siRNA with NP, NP-P and NP-F nanoparticles. Each nanoplex was formed with pDNA, dsODN or siRNA in water at various charge ratios (+/−) from 1/1 to 4/1, and analyzed using agarose gel for pDNA or acrylamide gel electrophoresis for dsODN and siRNA. O.C. indicates open circular pDNA; S.C. indicates supercoiled pDNA.

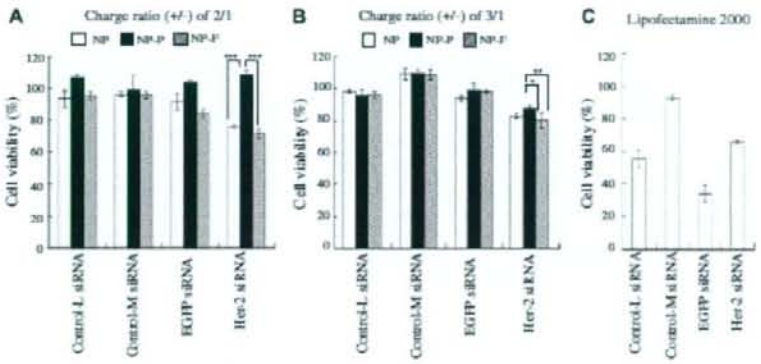

Fig. 2. Antiproliferative activity 72 h after transfection of Her-2 siRNA by nanoparticles into KB cells. Nanoplexes were prepared by mixing nanoparticles with siRNAs in 5 mM NaCl solution at a charge ratio (+/−) of 2/1 (A) or 3/1 (B). Lipofectamine 2000 lipoplex (C) was prepared according to the manufacturer's protocol. Each column represents the mean ± SD ($n = 3$). $^{*}P < 0.05$, $^{**}P < 0.01$ and $^{***}P < 0.001$ by one-way analysis of variance on ranks with Tukey–Kramer's post-hoc test.

of 2/1 and 3/1, and more significantly at 2/1. Each nanoplex of control-M, control-L and EGFP siRNA had no apparent effect on cell growth. The transfection of lipofectamine 2000 lipoplex with Her-2 siRNA strongly suppressed cell growth (66%), and those with control-L siRNA and EGFP siRNA also strongly induced the inhibition of cell growth by off-target effect (55% and 34%, respectively) (Fig. 2C). These findings suggested that the NP-F nanoplex of Her-2 siRNA at a charge ratio (+/−) of 2/1 could selectively suppress the growth of tumor cells without an off-targeting effect, but lipofectamine 2000 with Her-2 siRNAs strongly suppressed cell growth with an off-targeting.

3.3. Western blot analysis

To confirm whether the nanoplexes of Her-2 siRNA at a charge ratio (+/−) of 2/1 suppressed Her-2 expression, we assessed the expression of Her-2 protein in KB cells 72 h after transfection of nanoplexes of Her-2 siRNA by Western blotting. NP and NP-F nanoplexes inhibited the expression of Her-2, while NP-P nanoplex was insufficient (Fig. 3). All nanoplexes and the lipofectamine 2000 lipoplex of control-M siRNA did not affect the expression of Her-2 protein and β-actin as a control protein. These results showed clearly that NP-F nanoplex down-regulated targeted proteins strongly without off-target effects.

3.4. Size of nanoplex

To apply nanoplex to intratumoral injection, the size of nanoplexes formed in water, 5 and 10 mM NaCl solutions were measured. The size of NP nanoplex formed in water at a charge ratio (+/−) of 3/1 increased, but NP-P and NP-F nanoplex did not, suggesting that PEGylation of NP might stabilize its structure (Table 1). The sizes of NP, NP-P and NP-F nanoplex formed in 5 mM NaCl solution at a charge ratio (+/−) of 3/1 increased to about 300-

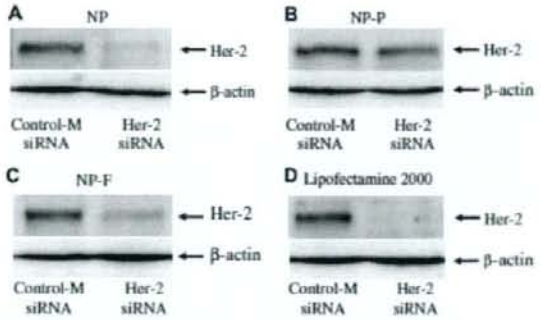

Fig. 3. Down-regulation of Her-2 protein expression by siRNA/NP nanoplexes. KB cells were treated with NP (A), NP-P (B), NP-F (C) nanoplex formed in 5 mM NaCl solution at a charge ratio (+/−) of 2/1 at a final concentration of 100 nM Her-2 or control-M siRNA. Lipofectamine 2000 lipoplex (D) was prepared according to the manufacturer's protocol. Levels of Her-2 and β-actin protein were evaluated by Western blotting 72 h after incubation.

Table 1
Size and ζ-potential of nanoplexes formed in water, 5 and 10 mM NaCl solution at various charge ratios (+/−)

	Charge ratio (+/−)	Size (nm) of nanoplex forming			ζ-potential (mV)
		In water	In 5 mM NaCl	In 10 mM NaCl	In water
NP	1/0	113.4 ± 1.1	95.4 ± 1.5	88.2 ± 6.3	54.3 ± 0.8
	1/1	104.3 ± 0.7	135.3 ± 1.1	596.1 ± 358.7	−20.0 ± 0.8
	2/1	107.2 ± 2.2	177.4 ± 4.6	382.2 ± 11.8	−19.6 ± 0.7
	3/1	322.8 ± 16.5	339.2 ± 0.7	145.2 ± 0.6	13.8 ± 2.5
NP-P	1/0	129.7 ± 0.9	116.5 ± 1.8	102.2 ± 2.0	47.7 ± 0.7
	1/1	125.2 ± 0.6	155.3 ± 0.4	110.4 ± 2.4	−24.4 ± 1.3
	2/1	139.4 ± 2.4	161.1 ± 1.5	339.4 ± 82.3	−21.6 ± 0.8
	3/1	132.8 ± 1.8	429.9 ± 26.0	311.3 ± 1.9	20.7 ± 1.3
NP-F	1/0	146.8 ± 2.3	123.3 ± 0.5	115.0 ± 1.3	49.3 ± 1.0
	1/1	151.7 ± 3.2	180.7 ± 2.4	169.8 ± 1.4	−28.8 ± 2.3
	2/1	144.4 ± 2.2	192.8 ± 2.7	183.1 ± 18.4	−9.4 ± 3.0
	3/1	144.7 ± 1.7	575.3 ± 17.8	482.6 ± 85.5	20.0 ± 1.7

Each value represents the mean ± SD (n = 3).

500 nm, but those in 10 mM NaCl solution increased at charge ratios (+/−) of above 1/1, 2/1 and 3/1, respectively. All nanoplexes remained small when formed in water or 5 mM NaCl at a charge ratio of 2/1, and became slightly larger at a charge ratio (+/−) of 3/1. This may be due to that the ζ-potential of each nanoplex was increased in parallel with the increasing charge ratio (+/−) and became positive at a charge ratio (+/−) of above 3/1 (Table 1). The cationic charge on the surface of the nanoplex may be neutralized by the presence of NaCl, resulting in instability of the nanoplex and facilitating the size increase. From the results of antiproliferative activity and injectable size of nanoplex, we used the nanoplexes formed in 5 mM NaCl at a charge ratio of 2/1 in subsequent experiments.

3.5. Association of FAM-labeled nanoplexes with KB cells

Next, to compare association with KB cells among nanoplexes formed in water or in NaCl solution, nanoplexes with FAM-labeled siRNA were studied by flow cytometry after 24 h incubation. The associations of all nanoplexes formed in 5 mM NaCl solution were found to be about 8–9-fold higher than those in water, respectively (Fig. 4). In NP-P nanoplex, the surface modification of NP with PEG resulted in reduced non-specific uptake; therefore, NP-P nanoplex exhibited lower cellular association. NP-F nanoplex may restore the interaction between the folate moiety of NP-F and FR of KB cells, exhibiting significantly higher cellular association than NP-P.

The results were consistent with the finding that lipoplexes prepared in 5 mM NaCl solution increased transfection efficiency [28,29], but it is not clear why the nanoplex formed in 5 mM NaCl enhanced cellular association. Usually, nanoplexes are prepared in non-ionic solution such as water or glucose solution because they aggregate in the presence of ionic solutions such as saline, however; the nanoplex formed in water was exposed to ionic solution such as culture medium or blood and subsequently increased in size or aggregate. Controlling the size of the nanoplex after exposure to ionic solution is important for efficient gene transfer. The presence of NaCl during nanoplex formation can regulate the repulsion between cationic nanoplexes [28]. This stabilized effect of nanoplex in ionic solution might increase cellular association.

3.6. Localization of siRNA transfected into KB cells

The intracellular localization of siRNA after transfection is crucial for its successful function as an inductor of the RNA interference process. pDNA must be transferred into the nucleus for the expression of transgenes, but siRNA does not need to enter the cell nucleus since the targets for siRNA applications are in the cytoplasm. To investigate whether siRNA after transfection localized

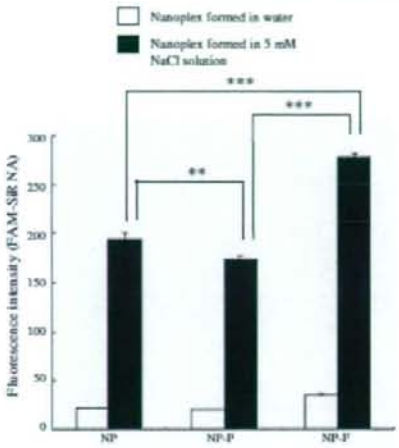

Fig. 4. Uptake of FAM-labeled siRNA by nanoparticles into KB cells 24 h after incubation by flow cytometry. NP, NP-P and NP-F nanoplexes at a charge ratio (+/−) of 2/1 were prepared by mixing FAM-labeled siRNA with each nanoparticle in the presence or absence of 5 mM NaCl solution. KB cells were incubated with these nanoplexes at a final concentration of 100 nM siRNA. Each column represents the mean ± SD ($n = 3$). $^{**}P < 0.01$ and $^{***}P < 0.001$ by one-way analysis of variance on ranks with Tukey–Kramer's post-hoc test.

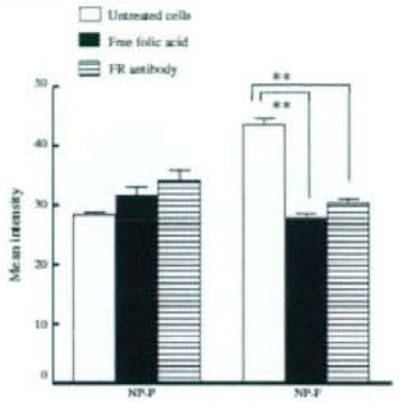

Fig. 6. Competition analysis of NP-F nanoplex with KB cells by flow cytometry. KB cells were incubated for 1 h in the absence or presence of 1 mM free folic acid or 20 μg/ml FR antibody. DiI-labeled NP-P or NP-F was mixed with siRNA at a charge ratio (+/−) of 2/1 in 5 mM NaCl. Nanoplexes were incubated with cells for another 3 h. The results indicate the mean ± SD ($n = 3$).

in cytoplasm where RNAi occurs, we examined the localization of FAM-labeled siRNA in cells 24 h after transfection. When NP and NP-F nanoplex was transfected into cells, FAM-labeled siRNA was

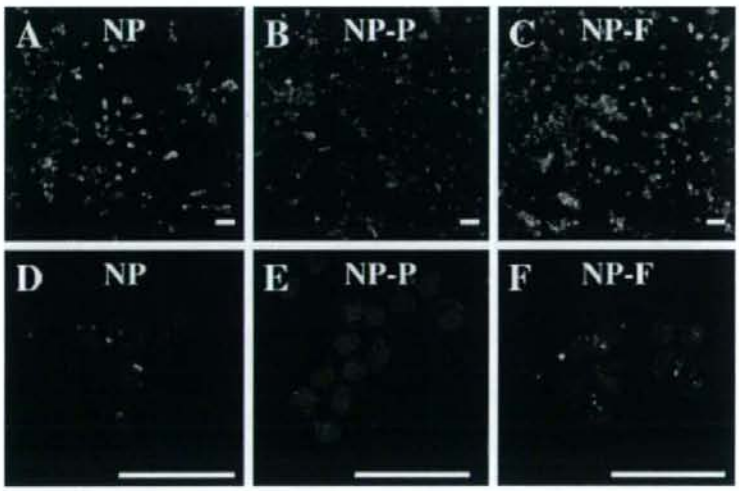

Fig. 5. Intracellular localization of FAM-labeled siRNA 24 h after incubation with KB cells by confocal laser-scanning microscope. FAM-labeled siRNA was complexed with NP, NP-P and NP-F, respectively, at a charge ratio (+/−) of 2/1 in 5 mM NaCl and then diluted to 100 nM siRNA with medium. ×200 (A–C) or ×1200 (D–F) magnification. Nuclei were stained by propidium iodide. Scale bar = 50 μm.

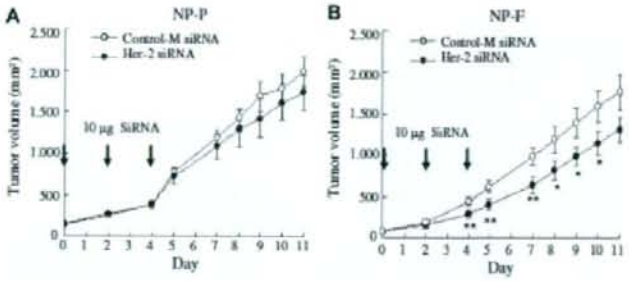

Fig. 7. *In vivo* gene therapy of KB tumor xenografts with Her-2 siRNA in mice. Mice were divided into two groups: group I, control-M siRNA(10 μg) as a control; group II, Her-2 siRNA (10 μg). NP-P (A) or NP-F nanoplexes (B) of siRNAs formed at a charge ratio(+/−) of 2/1 in 5 mM NaCl were injected directly into the tumor three times (days 0, 2 and 4). The results indicate the mean ± SE ($n = 4$–6). $^{*}P < 0.05$ and $^{**}P < 0.01$, compared with control-M siRNA by Student's *t*-test.

found in most of the cells (Fig. 5A and C) and in the cellular cytoplasm and nucleus (Fig. 5D and F), however; when NP-P was transfected, signals were hardly detected in the cells (Fig. 5E). This suggested that NP-F could efficiently transfer siRNA into the cells.

3.7. Competition analysis of NP-F nanoplex with KB cells

To further examine the selectivity of NP-F to carry genes into KB cells, we measured the association of a non-exchangeable fluorescent membrane probe, DiI-labeled NP-F complexed with siRNA, by flow cytometry. As shown in Fig. 6, competitive experiments in the presence of folic acid or FR antibody revealed a largely decreased amount of NP-F in the cells compared with NP-P. These results clearly indicated that the association of NP-F nanoplex with KB cells occurred *via* FR.

3.8. *In vivo* gene therapy in KB tumor xenografts

Finally, we evaluated the antitumor effect by direct injection into KB tumor xenografts with the NP-F nanoplex of Her-2 siRNA. The growth of KB tumors was not inhibited in mice treated with the NP-P nanoplex of Her-2 siRNA compared with control-M siRNA (Fig. 7A). However, the growth was significantly inhibited in mice treated with the NP-F nanoplex of Her-2 siRNA on day 4, 5, 7, 8, 9 and 10 compared with control-M siRNA (Fig. 7B).

Lipofectamine 2000 lipoplexes induced undesired inhibition in control siRNAs by an off-targeting effect in *in vitro* transfection (Fig. 2C), and could not be available for *in vivo* transfection. In contrast, the NP-F nanoplex of Her-2 siRNA could significantly inhibit *in vitro* growth of tumor cells without an off-targeting effect (Fig. 2A), and also suppress *in vivo* growth of tumor xenografts (Fig. 7B). Thus, NP-F is more appropriate for siRNA delivery than lipofectamine 2000 from the aspects of off-targeting effect and *in vivo* application. However, complete regression of tumor was not observed in the xenografts transfected with Her-2 siRNA by the NP-F nanoplex. In *in vitro* study, transfection with Her-2 siRNA could suppress expression of Her-2 protein (Fig. 3) and cell growth, but not lead to complete cell death (Fig. 2A). Her-2 activates cell survival pathways, which represents an advantage for tumor cells as they became resistant to chemotherapy-induced apoptosis [31,32]. Down-regulation of Her-2 expression in tumor cells leads to an activation of apoptosis pathway and enhances cytotoxicity by chemotherapy [33,34]. Therefore, for complete regression of tumor, a combination therapy with Her-2 siRNA and chemotherapy might be needed.

4. Conclusions

In this study, we showed that folate-linked nanoparticles delivered synthetic siRNA with high transfection efficiency and selectivity into nasopharyngeal tumor KB cells by forming a nanoplex in NaCl solution. In *in vitro* experiments, the association of NP-F nanoplex with the cells occurred *via* FR, and NP-F nanoplex of Her-2 siRNA suppressed the cell viability. In *in vivo*, the NP-F nanoplexes with Her-2 siRNA by intratumoral injection significantly suppressed the growth of KB xenografts in mice, compared with NP-P nanoplexes. These findings suggest that folate-linked nanoparticles have potential as a clinically effective vector in nasopharyngeal cancer synthetic siRNA gene therapy.

Acknowledgements

This project was supported in part by a Grant-in Aid for Scientific Research from the Ministry of Education, Culture, Sports, Science, and Technology of Japan, and by the Open Research Center Project.

References

[1] A. Fire, S. Xu, M.K. Montgomery, S.A. Kostas, S.E. Driver, C.C. Mello, Potent and specific genetic interference by double-stranded RNA in Caenorhabditis elegans, Nature 391 (1998) 806–811.
[2] S.M. Elbashir, J. Harborth, W. Lendeckel, A. Yalcin, K. Weber, T. Tuschl, Duplexes of 21-nucleotide RNAs mediate RNA interference in cultured mammalian cells, Nature 411 (2001) 494–498.
[3] J. Yano, K. Hirabayashi, S. Nakagawa, T. Yamaguchi, M. Nogawa, I. Kashimori, H. Naito, H. Kitagawa, K. Ishiyama, T. Ohgi, T. Irimura, Antitumor activity of small interfering RNA/cationic liposome complex in mouse models of cancer, Clin. Cancer Res. 10 (2004) 7721–7726.
[4] T.R. Brummelkamp, R. Bernards, R. Agami, Stable suppression of tumorigenicity by virus-mediated RNA interference, Cancer Cell 2 (2002) 243–247.
[5] C. Lois, Y. Refaeli, X.F. Qin, L. Van Parijs, Retroviruses as tools to study the immune system, Curr. Opin. Immunol. 13 (2001) 496–504.
[6] S. Lu, B.R. Cullen, Adenovirus VA1 noncoding RNA can inhibit small interfering RNA and MicroRNA biogenesis, J. Virol. 78 (2004) 12868–12876.
[7] H. Uchida, T. Tanaka, K. Sasaki, K. Kato, H. Dehari, Y. Ito, M. Kobune, M. Miyagishi, K. Taira, H. Tahara, H. Hamada, Adenovirus-mediated transfer of siRNA against survivin induced apoptosis and attenuated tumor cell growth in vitro and in vivo, Mol. Ther. 10 (2004) 162–171.
[8] G.J. Arts, E. Langereijer, R. Tiesinga, L. Ma, H. Pavliska, K. Dolic, R. Dooijes, E. Mesic, R. Claeys, F. Michiels, S.J. van der, M. Lambrechts, S. Herman, R. Reys, K. Thys, M. Hoffmann, P. Tomme, H. van Es, Adenoviral vectors expressing siRNAs for discovery and validation of gene function, Genome Res. 13 (2003) 2325–2332.
[9] T. Abbas-Terki, W. Blanco-Bose, N. Deglon, W. Pralong, P. Aebischer, Lentiviral-mediated RNA interference, Hum. Gene Ther. 13 (2002) 2197–2206.

[10] A.M. Diaz, K. Bernardo, Reversal of senescence in mouse fibroblasts through lentiviral suppression of p53, J. Biol. Chem. 278 (2003) 11731–11734.
[11] D.A. Robinson, C.F. Dillon, A.V. Kwiatkowski, C. Sievers, L. Yang, J. Kopinja, D.L. Rooney, M.M. Ihrig, M.T. McManus, F.B. Gertler, M.L. Scott, L. Van Parijs, A lentivirus-based system to functionally silence genes in primary mammalian cells, stem cells and transgenic mice by RNA interference, Nat. Genet. 33 (2003) 401–406.
[12] A.P. McCaffrey, L. Meuse, T.T. Pham, D.S. Conklin, G.J. Hannon, M.A. Kay, RNA interference in adult mice, Nature 418 (2002) 38–39.
[13] D.R. Sorensen, M. Leirdal, M. Sioud, Gene silencing by systemic delivery of synthetic siRNAs in adult mice, J. Mol. Biol. 327 (2003) 761–766.
[14] D.L. Lewis, J.K. Hagstrom, A.G. Loomis, J.A. Wolff, H. Herweijer, Efficient delivery of siRNA for inhibition of gene expression in postnatal mice, Nat. Genet. 32 (2002) 107–108.
[15] F. Takeshita, Y. Minakuchi, S. Nagahara, K. Honma, H. Sasaki, K. Hirai, T. Teratani, N. Namatame, Y. Yamamoto, K. Hatai, T. Kato, A. Sano, T. Ochiya, Efficient delivery of small interfering RNA to bone-metastatic tumors by using atelocollagen in vivo, Proc. Natl. Acad. Sci. USA 102 (2005) 12177–12182.
[16] Y. Minakuchi, F. Takeshita, N. Kosaka, H. Sasaki, Y. Yamamoto, M. Kouno, K. Honma, S. Nagahara, K. Hanai, A. Sano, T. Kato, M. Terada, T. Ochiya, Atelocollagen-mediated synthetic small interfering RNA delivery for effective gene silencing in vitro and in vivo, Nucleic Acids Res. 32 (2004) e109.
[17] P.Y. Chien, J. Wang, D. Carbonaro, S. Lei, B. Miller, S. Sheikh, S.M. Ali, M.U. Ahmad, I. Ahmad, Novel cationic cardiolipin analogue-based liposome for efficient DNA and small interfering RNA delivery in vitro and in vivo, Cancer Gene Ther. 12 (2005) 321–328.
[18] J.F. Ross, P.K. Chaudhuri, M. Ratnam, Differential regulation of folate receptor isoforms in normal and malignant tissues in vivo and in established cell lines. Physiologic and clinical implications, Cancer 73 (1994) 2432–2443.
[19] N. Parker, M.J. Turk, E. Westrick, J.D. Lewis, P.S. Low, C.P. Leamon, Folate receptor expression in carcinomas and normal tissues determined by a quantitative radioligand binding assay, Anal. Biochem. 338 (2005) 284–293.
[20] O.C. Farokhzad, J. Cheng, B.A. Teply, I. Sherifi, S. Jon, P.W. Kantoff, J.P. Richie, R. Langer, Targeted nanoparticle-aptamer bioconjugates for cancer chemotherapy in vivo, Proc. Natl. Acad. Sci. USA 103 (2006) 6315–6320.
[21] A. Nori, J. Kopecek, Intracellular targeting of polymer-bound drugs for cancer chemotherapy, Adv. Drug Deliv. Rev. 57 (2005) 609–636.
[22] J.W. Park, K. Hong, D.B. Kirpotin, G. Colbern, R. Shalaby, J. Baselga, Y. Shao, U.B. Nielsen, J.D. Marks, D. Moore, D. Papahadjopoulos, C.C. Benz, Anti-HER2 immunoliposomes: enhanced efficacy attributable to targeted delivery, Clin. Cancer Res. 8 (2002) 1172–1181.
[23] H.S. Yoo, T.G. Park, Folate receptor targeted biodegradable polymeric doxorubicin micelles, J. Control Release 96 (2004) 273–283.
[24] K.S. Hwa, J.J. Heon, C.K. Chul, K.S. Wan, P.T. Gwan, Target-specific gene silencing by siRNA plasmid DNA complexed with folate-modified poly(ethylenimine), J. Control Release 104 (2005) 223–232.
[25] S.H. Kim, H. Mok, J.H. Jeong, S.W. Kim, T.G. Park, Comparative evaluation of target-specific GFP gene silencing efficiencies for antisense ODN synthetic siRNA, and siRNA plasmid complexed with PEI–PEG–FOL conjugate, Bioconjug. Chem. 17 (2006) 241–244.
[26] Y. Hattori, H. Kubo, K. Higashiyama, Y. Maitani, Folate-linked nanoparticles formed with DNA complexes in sodium chloride solution enhance transfection efficiency, J. Biomed. Nanotech. 1 (2005) 176–184.
[27] Y. Hattori, Y. Maitani, Enhanced in vitro DNA transfection efficiency by novel folate-linked nanoparticles in human prostate cancer and oral cancer, J. Control Release 97 (2004) 173–183.
[28] S. Fumoto, S. Kawakami, Y. Ito, K. Shigeta, F. Yamashita, M. Hashida, Enhanced hepatocyte-selective in vivo gene expression by stabilized galactosylated liposome/plasmid DNA complex using sodium chloride for complex formation, Mol. Ther. 10 (2004) 719–729.
[29] S. Kawakami, Y. Ito, S. Fumoto, F. Yamashita, M. Hashida, Enhanced gene expression in lung by a stabilized lipoplex using sodium chloride for complex formation, J. Gene Med. 7 (2005) 1526–1533.
[30] N.E. Hynes, H.A. Lane, ERBB receptors and cancer: the complexity of targeted inhibitors, Nat. Rev. Cancer 5 (2005) 341–354.
[31] L.M. Witters, S.M. Santala, L. Engle, V. Chinchilli, A. Lipton, Decreased response to paclitaxel versus docetaxel in HER-2/neu transfected human breast cancer cells, Am. J. Clin. Oncol. 26 (2003) 50–54.
[32] R. Kumar, M. Mandal, A. Lipton, H. Harvey, C.R. Thompson, Overexpression of HER2 modulates bcl-2, bcl-XL and tamoxifen-induced apoptosis in human MCF-7 breast cancer cells, Clin. Cancer Res. 2 (1996) 1215–1219.
[33] P.J. Real, A. Benito, J. Cuevas, M.T. Berciano, J.A. de, P. Coffer, J. Gomez-Roman, M. Lafarga, J.M. Lopez-Vega, J.L. Fernandez-Luna, Blockade of epidermal growth factor receptors chemosensitizes breast cancer cells through up-regulation of Bcl-XL, Cancer Res. 65 (2005) 8151–8157.
[34] X. Hu, F. Su, L. Qin, W. Jia, C. Gong, F. Yu, J. Guo, E. Song, Stable RNA interference of Erbb-2 gene synergistic with epirubicin suppresses breast cancer growth in vitro and in vivo, Biochem. Biophys. Res. Commun. 346 (2006) 778–785.

NaCl Induced High Cationic Hydroxyethylated Cholesterol-Based Nanoparticle-Mediated Synthetic Small Interfering RNA Transfer into Prostate Carcinoma PC-3 Cells

Yoshiyuki HATTORI,* Takashi YOSHIZAWA, Kimiko KOGA, and Yoshie MAITANI

Institute of Medicinal Chemistry, Hoshi University; 2–4–41 Ebara, Shinagawa-ku, Tokyo 142–8501, Japan.
Received May 14, 2008; accepted October 6, 2008; published online October 8, 2008

The RNA interference (RNAi) effect is an alternative technology to antisense DNA as an experimental method of down-regulating a specific target protein. Optimal gene therapy for tumors must deliver synthetic small interfering RNA (siRNA) to tumor cells with high efficiency and minimal toxicity. Previously, we reported that cationic nanoparticles composed of cholesteryl-3β-carboxyamidoethylene-*N*-hydroxyethylamine and Tween 80 (NP-OH) could deliver plasmid DNA with high transfection efficiency. In this study, to apply NP-OH for siRNA transfection, we optimized the charge ratio (+/−) of NP-OH/siRNA and nanoplex-forming solution, and evaluated the transfection efficiency into PC-3 cells. Positively charged nanoplex prepared in the presence of sodium chloride exhibited efficient siRNA transfer. The distribution of siRNA after transfection was strongly detected both in the cytoplasm and nucleus. Furthermore, we demonstrated that NP-OH nanoplex of bcl-2 siRNA significantly inhibited tumor growth compared with control siRNA, and the efficacy was comparable to commercial products. The results of the experiments showed that NP-OH nanoparticles have potential as a viable vector candidate for synthetic siRNA delivery.

Key words cationic nanoparticle; synthetic small interfering RNA; RNA delivery; cholesteryl-3β-carboxyamidoethylene-*N*-hydroxyethylamine; nanoplex; PC-3 cell

RNA interference (RNAi) is a powerful gene-silencing process that holds great promise in the field of cancer therapy.[1] RNAi can be induced in mammalian cells by the introduction of synthetic small interfering RNA (siRNA) consisting of 19—27 base pairs in length or by plasmid DNA (pDNA) that expresses short hairpin RNAs (shRNA) that are subsequently processed to siRNA by cellular machinery.[2—4] Synthetic siRNAs, which are small double-stranded RNA, are substrates for the RNA-induced silencing complex.[2] siRNA suppresses the expression of a target gene by triggering specific degradation of the complementary mRNA sequence. siRNAs are expected to have a medicinal application in human gene therapy as drugs with high specificity for molecular targeting; however, the methods of delivering synthetic siRNA in human therapy are still an unresolved issue.

Viral vectors like retrovirus-,[5,6] adenovirus-[7—9] and lentivirus-based vectors[10—12] have been successful in obtaining efficient and long gene silencing using siRNA. Among them, adenoviral vectors are widely used both *in vitro* and *in vivo*; however, they possess high immunogenicity and pro-inflammatory effects. As alternative delivery technologies, non-viral vectors have been developed, among which cationic liposomes and nanoparticles have mostly been investigated, but this is still at a preliminary level. Although cationic liposomes for *in vitro* delivery of siRNA are used, the success of *in vivo* siRNA delivery has been limited compared with that of the pDNA delivery. The optimized liposome formulation for siRNA delivery is different from that for pDNA delivery[13]; therefore, the first approach to develop cationic lipid based vector-mediated siRNA delivery to cells was to determine a cationic lipid for optimal interaction with siRNA.

Many different cationic lipids have been synthesized for delivering genes into cells. The use of cationic cholesterol derivatives could be justified by their high transfection activity and low toxicity.[14,15] Cationic cholesterol derivatives are composed of three distinct parts: a cholesteryl skeleton, a cationic amino group and a linker arm between the cholesteryl skeleton and cationic amino group. Derivatives with different combinations of these parts were reported and some have high transfection efficiency.[14—16] Among them, cholesteryl-3β-carboxyamidoethylene-*N*-hydroxyethylamine (OH-Chol) is a cationic lipid with a hydroxyethyl group at the amino terminal, showing the most efficient transfection efficiency for pDNA and antisense oligodeoxynucleotide (AS-ODN) delivery.[17,18]

We previously reported that cationic nanoparticles (NP-OH) containing OH-Chol could deliver pDNA with high transfection efficiency *in vitro* when the nanoparticle/pDNA complex (nanoplex) was formed in 50 mM NaCl solution.[19] In this study, to apply NP-OH for a synthetic siRNA transfection vector, we optimized the charge ratio (+/−) of NP-OH/siRNA and nanoplex-forming solution, and evaluated transfection efficiency into PC-3 cells. Furthermore, we investigated the growth inhibition of tumor cells by a synthetic siRNA for bcl-2 mRNA with NP-OH.

MATERIALS AND METHODS

Plasmid DNA and siRNA The plasmid pCMV-Gluc control encoding secretable *Gaussia* luciferase (Gluc) under the control of the cytomegalovirus (CMV) promoter was purchased from New England Biolabs (MA, U.S.A.). A protein-free preparation of these plasmids was purified following alkaline lysis using maxiprep columns (Qiagen, Hilden, Germany).

The siRNAs targeting nucleotides of Gluc and enhanced green fluorescent protein (EGFP) mRNA or random siRNA as a negative control were synthesized by Hokkaido System Science (Hokkaido, Japan). Gluc siRNA sense strand, 5′-GAGAACAACGAAGACUUCAACAUCGAG-3′ and Gluc siRNA antisense strand, 5′-CGAUGUUGAAGUCUUCGUUGUUCUCAU-3′; EGFP siRNA sense strand, 5′-ACGGC-

* To whom correspondence should be addressed. e-mail: yhattori@hoshi.ac.jp

AUCAAGGUGAACUUCAAGAUAG-3′ and EGFP siRNA antisense strand, 5′-AUCUUGAAGUUCACCUUGAUGC-CGUAU-3′; random siRNA sense strand, 5′-CGAUUCGCU-AGACCGGCUUCAUUGCAG-3′ and random siRNA antisense strand, 5′-GCAAUGAAGCCGGUCUAGCGAAUCG-AU-3′. 5′-Carboxyfluorescein (FAM)-labeled random siRNA was used to determine the amount of cellular uptake.

The stealth RNA interference duplex-targeting nucleotides of bcl-2 mRNA (bcl-2 siRNA), stealth RNAi Negative Control Kit with Medium GC as a control for bcl-2 siRNA (negative control siRNA) and Alexa Fluor 555-labeled siRNA (BLOCK-iT Alexa Fluor Red Fluorescent Oligo) were synthesized by Invitrogen (Carlsbad, CA, U.S.A.). The stealth siRNAs are chemically modified to increase the specificity by allowing only the antisense strand to efficiently enter the RNAi pathway and eliminating induction of interferon-related pathways. The siRNA sequences of the bcl-2 were bcl-2a sense strand: 5′-ACUCAAAGAAGGCCACAAUCCUC-CC-3′ and antisense strand 5′-GGGAGGAUUGUGGCC-UUCUUUGAGU-3′, bcl-2b: sense strand 5′-UACUCAG-UCAUCCACAGGGCGAUGU-3′ and antisense strand 5′-ACAUCGCCCUGUGGAUGACUGAGUA-3′, bcl-2c: sense strand 5′-UUAUCCUGGAUCCAGGUGUGCAGGU-3′ and antisense strand 5′-ACCUGCACACCUGGAUCCAGGAU-AA-3′. The bcl-2 siRNA is used as a cocktail of three duplexes (100 nmol of bcl-2 siRNA cocktail containing 33.3 nmol of each individual siRNA).

Preparation and Size of Nanoparticles and Nanoplexes OH-Chol was synthesized as previously described.[19] DC-Chol was purchased from Sigma Chemical Co. (St. Louis, MO, U.S.A.). Tween 80 was obtained from NOF Co., Ltd. (Tokyo, Japan). The OH-Chol-based nanoparticle, NP-OH, consisted of 1 mg/ml OH-Chol as a cationic lipid, and 5 mol% Tween 80, and the DC-Chol-based nanoparticle, NP-DC, consisted of 1 mg/ml DC-Chol and 5 mol% Tween 80. Each nanoparticle was prepared with lipids (*e.g.* OH-Chol : Tween 80 = 10 : 1.3, weight (mg)) in 10 ml water by the modified ethanol injection method as previously described.[19]

The nanoparticle/siRNA complex (nanoplex) at various charge ratios (+/−) of cationic lipid to siRNA was formed by the addition of each nanoparticle to 100 pmol siRNA in water or 50 μl of 5—50 mM NaCl solution with gentle shaking and leaving at room temperature for 10 min. In stability of nanoplex in culture medium, the size of nanoplex was measured after incubation of the nanoplex with RPMI-1640 medium for a further 15 min at room temperature (Life Technologies, Inc., Grand Island, NY, U.S.A.). The particle size distributions and ζ-potentials were measured by ELS-Z2 (Otsuka Electronics Co., Ltd., Osaka, Japan) at 25 °C after diluting the dispersion to an appropriate volume with water. The average size and ζ-potential of NP-OH were approximately 120—130 nm and +45—50 mV, respectively.

Gel Electrophoresis One microgram of siRNA was mixed with aliquots of NP-OH or NP-DC (1 to 4 charge equivalent of cationic lipid) in the presence or absence of various concentrations of NaCl solution. After 10 min incubation of the nanoplexes, they were analyzed by 12% acrylamide gel electrophoresis in Tris–Borate–EDTA (TBE) buffer and visualized by ethidium bromide staining as previously described.[19]

Cell Culture PC-3 cells were supplied by the Cell Resource Center for Biomedical Research, Tohoku University (Miyagi, Japan). The cells were grown in RPMI-1640 medium (Invitrogen) supplemented with 10% heat-inactivated fetal bovine serum (FBS) (Invitrogen) and kanamycin (100 μg/ml) at 37 °C in a 5% CO_2 humidified atmosphere.

For the preparation of PC-3 cells stably expressing Gluc, PC-3 cells were plated on 35-mm culture dishes. Twenty-four hours later, the cells were transfected with 2 μg of pCMV-Gluc using lipofectamine 2000 reagents. The transfected cells were selected in medium with 800 μg/ml G418 sulfate for 2 weeks. G418-resistant colonies were subcultured and established as a permanent cell line transduced with pCMV-Gluc (PC-3-Gluc) and were used for subsequent experiments.

Confocal Microscopy PC-3 cells were plated on 35-mm culture dishes. NP-OH was mixed with 100 pmol of Alexa Fluor 555-labeled siRNA at a charge ratio (+/−) of 3/1 in water, 5, 20, or 50 mM NaCl and incubated for 10 min. The mixtures were diluted to 100 nM with 1 ml of medium supplemented with 10% serum, and incubated with the cells for 24 h. After incubation, cells were washed twice with phosphate-buffered saline (PBS) and fixed with 4% formaldehyde in PBS for 30 min at room temperature. Examinations were performed with a Radiance 2100 confocal laser scanning microscope (BioRad, CA, U.S.A.) as previously described.[20] Alexa Fluor 555-labeled siRNA in the cells was imaged using a 543-nm internal He–Neon laser for excitation, and fluorescence emission was observed with a filter, 560DCLP.

Gluc Assay PC-3-Gluc cells were plated on 96-well culture dishes. For transfection, each NP-OH and NP-DC nanoplex of siRNA was diluted in 1 ml of medium supplemented with 10% FBS and then incubated with the cells for 24 h or 48 h. Lipofectamine 2000 lipoplex was prepared according to the manufacturer's protocol and then incubated with the cells for 24 or 48 h. The level of Gluc activity was evaluated by luciferase activity in the medium, which was measured as counts per second (cps)/culture medium (ml) using a *Gaussia* Luciferase Assay Kit (New England BioLabs, Inc., MA, U.S.A.). Gluc activity (%) was calculated as relative to the Gluc activity (cps/ml) of untransfected cells.

Flow Cytometric Analysis PC-3 cell cultures were prepared by plating the cells on a 35-mm culture dish 24 h prior to each experiment. For the experiment of siRNA uptake, NP-OH was mixed with 100 pmol of 5′FAM-labeled siRNA in water or 5—50 mM NaCl at a charge ratio (+/−) of 3/1. The nanoplexes were then diluted to 100 nM with 1 ml of medium containing 10% FBS and added to the cell. After 24 h incubation, the dish was washed 2 times with 1 ml of PBS (pH 7.4) to remove any unbound nanoplex, and the cells were detached with 0.05% trypsin. The amount of FAM-labeled siRNA in the cells was determined by examining fluorescence intensity on a FACSCalibur flow cytometer (Becton Dickinson, San Jose, CA, U.S.A.) as previously described.[20]

Cytotoxicity PC-3 cells were plated on 35-mm culture dishes. NP-OH was mixed with 100 pmol of negative control siRNA at various charge ratios (+/−) in 50 mM NaCl and incubated for 10 min. The mixtures were diluted to 100 or 50 nM with medium supplemented with 10% serum, and incubated with the cells for 24 h. After incubation, the cells were washed and incubated with propidium iodide (PI) for 10 min at 37 °C. PI staining of the cellular nucleus was used

as a marker for cell death. Dead cells were visualized with an Eclipse TS100-F (Nikon, Tokyo, Japan).

Antiproliferative Activity Antiproliferative activity upon transfection of bcl-2 siRNA, negative control and EGFP siRNA using NP-OH or lipofectamine 2000 was evaluated with a cell proliferation assay kit (Dojindo, Kumamoto, Japan). PC-3 cells were placed on a 96-well plate in medium containing 10% FBS, and were transfected at 100 or 50 nM siRNA of nanoplex formed at a charge ratio (+/−) of 3/1 in the presence of 50 mM NaCl solution. After 48 h of incubation, the medium was removed, and the cells were treated with WST-8 (2-(2-methoxy-4-nitrophenyl)-3-(4-nitrophenyl)-5-(2,4-disulfophenyl)-2*H*-tetrazolium, monosodium salt) solution (10 μl) in medium containing serum (100 μl) for 30 min. Cell viability was expressed as relative to the absorbance at 450 nm of untransfected cells.

Detection of Protein Expression by Western Blotting PC-3 cells were seeded in a 35-mm culture dish and incubated overnight. The cells were transfected with bcl-2, negative control or EGFP siRNA, and then incubated for 48 h. The cells were suspended in lysis buffer (1% Triton-X 100 in PBS), and then centrifuged at 15000 rpm for 10 min. The supernatants (10 μg protein) were resolved on a 12% sodium dodecyl sulphate-polyacrylamide gel by electrophoresis (SDS-PAGE) and transferred to a polyvinylidene difluoride (PVDF) membrane (FluoroTrans® W, PALL Gelman Laboratory, Ann Arbor, MI, U.S.A.). The expression of Bcl-2 protein was identified using a specific rabbit antiserum (Stressgen Bioreagents, BC, Canada). The goat anti-rabbit IgG peroxidase conjugate (Santa Cruz Biotechnology, Inc., Santa Cruz, CA, U.S.A.) was used as a secondary antibody. Bcl-2 protein was detected with peroxidase-induced chemiluminescence (Super Signal West Pico Chemiluminescent Substrate, Pierce).

Quantitative PCR Analysis PC-3 cell cultures were prepared by plating the cells on a 35-mm culture dish 24 h prior to each experiment. NP-OH was mixed with 100 pmol of siRNA in 50 mM NaCl at a charge ratio (+/−) of 3/1. The nanoplexes were then diluted to 100 nM with 1 ml of medium containing 10% FBS and added to the cell. After 48 h incubation, total RNA was isolated from the cells and quantitative RT-PCR was performed on iCycler MyiQ detection systems (Bio-Rad Laboratories, Hercules, CA, U.S.A.) and SYBR Green I assay (iQ™ SYBER Green Supermix, Bio-Rad Laboratories) as described previously.[21] For the amplification of human bcl-2 cDNA, the primers bcl-2-FW, 5′-GATTGATGGGATCGTTGCCTTA-3′, and bcl-2-RW, 5′-CCTTGGCATGAGATGCAGGA-3′, were used. For the amplification of human β-actin cDNA, the primers β-actin-FW, 5′-TGGCACCCAGCACAATGAA-3′, and β-actin-RW, 5′-CTAAGTCATAGTCCGCCTAGAAGCA-3′, were used. Samples were run in triplicate and the expression level of bcl-2 mRNA was normalized for the amount of β-actin in the same sample. Difference of 1 cycle was calculated as a 2 fold-change in the gene expression.

Statistical Analysis The statistical significance of differences between mean values was determined by using Student's *t*-test. Multiple measurement comparisons were performed by analysis of variance followed by one-way analysis of variance on ranks with *post-hoc* Tukey–Kramer's test. A p value of 0.05 or less was considered significant.

RESULTS

Gel Retardation Assay To evaluate NP-OH for its ability to deliver siRNA to cells, we prepared nanoplexes at various charge ratios (+/−), and examined the association of siRNA with NP-OH by gel electrophoresis. The migration pattern of siRNA in the nanoplex changed when siRNA was mixed with NP-OH at charge ratios (+/−) from 1/1 to 4/1 in water. Beyond a charge ratio (+/−) of 3/1, no migration was observed (Fig. 1A). These results indicated that nanoplex was completely formed in water above a charge ratio (+/−) of 3/1. When NP-OH nanoplex at a charge ratio (+/−) of 3/1 was formed in the presence of various concentrations of NaCl, dissociation of siRNA from the nanoplex was not observed (Fig. 1B), indicating that the presence of NaCl in forming the nanoplex did not affect the association.

Suppression of Gluc Activity by Gene Knockdown Next, we prepared the NP-OH nanoplex at a charge ratio (+/−) of 3/1 in various concentrations of NaCl, and measured the transfection efficiencies of NP-OH into PC-3-Gluc cells by assaying Gluc activity 48 h after transfection in the presence of serum. The results showed that efficient siRNA

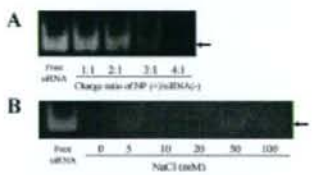

Fig. 1. Association of siRNA with NP-OH at Various Charge Ratios (+/−) in Water (A) and at a Charge Ratio (+/−) of 3/1 in Various Concentrations of NaCl (B) Was Analyzed Using Acrylamide Gel Electrophoresis

One microgram of siRNA was mixed with aliquots of NP-OH at various charge ratios (+/−) in water (A) or at a charge ratio (+/−) of 3/1 in various concentrations of NaCl (B). In A, charge ratios (+/−) of nanoparticle : siRNA=1 : 1, 2 : 1, 3 : 1 and 4 : 1

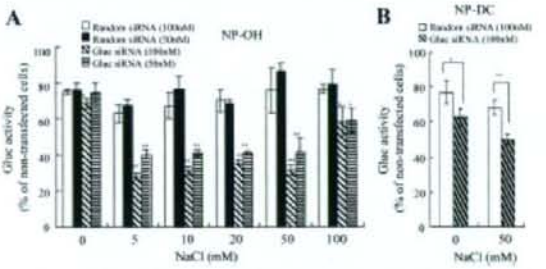

Fig. 2. Effect of NaCl Concentration in Forming Nanoplex on Transfection in PC-3-Gluc Cells 48 h after Transfection

NP-OH (A) or NP-DC (B) nanoplexes at a charge ratio (+/−) of 3/1 were prepared by mixing siRNA with NP-OH or NP-DC. Each column represents the mean ± S.D. (n=3). Statistical significance was evaluated by Student's *t* test. * $p<0.05$ and ** $p<0.01$, compared with nanoplex of random siRNA.

transfer depended on the formation condition of the nanoplex. When the NP-OH nanoplex of Gluc siRNA was formed in water, suppression of Gluc activity by Gluc siRNA was slightly observed in the cells (Fig. 2A). When NP-OH nanoplex was formed in 5—50 mM NaCl, suppression of Gluc activity was significantly observed at 100 and 50 nM Gluc siRNAs ($p<0.01$, compared with the nanoplex of random siRNA), but when that formed in 100 mM NaCl, it was only slightly.

We compared the transfection activity by NP-OH with that by the formulation of DC-Chol with Tween 80 (NP-DC). DC-Chol has often been used as a cationic lipid for vector. In NP-DC, suppression of Gluc activity was also slightly increased when NP-DC nanoplex was formed in 50 mM NaCl (Fig. 2B). The presence of 50 mM NaCl both in forming NP-OH and NP-DC nanoplexes increased the transfection activity of Gluc siRNA; however, NP-OH could suppress Gluc activity stronger than NP-DC. This finding indicated that NP-OH-based nanoparticles were more effective synthetic siRNA vector than NP-DC-based ones.

Uptake and Intracellular Localization of Transfected Synthetic siRNA To clarify the effect of nanoplex formation in 5–50 mM NaCl on transfection efficiency, we examined the cellular association of nanoplexes in the presence of serum by flow cytometric analysis. NP-OH nanoplexes were about 220, 340, 380, 790 and 1100 nm in size when formed in water and 5, 10, 20 and 50 mM NaCl solution, respectively (data not shown). Cellular association with the NP-OH nanoplex of FAM-labeled siRNA 24 h after transfection was significantly increased when the NP-OH nanoplex was formed in the presence of 5—50 mM NaCl (Figs. 3A, B). These findings seemed to correspond to the result of the suppression of Gluc activity (Fig. 2A).

Next, we examined the localization of Alexa Fluor 555-labeled siRNA 24 h after transfection into PC-3 cells by confocal microscopy. The distribution of siRNA was strongly detected both in the cytoplasm and nucleus using NP-OH nanoplex formed in 5—50 mM NaCl, but weakly in the cytoplasm when formed in water (Fig. 3C), suggesting that NP-OH nanoplex formed in NaCl could efficiently transfer siRNA into the cytoplasm. In subsequence experiments, we used 50 mM NaCl in forming the nanoplex as the concentration of NaCl.

Effect of Charge Ratio (+/−) of NP-OH/siRNA on Nanoplex Size To examine the effect of various NP-OH/siRNA ratios on transfection efficiency to cells, we examined the physicochemical properties of nanoplexes formed at various charge ratios (+/−) in water or NaCl solution. When NP-OH nanoplex was formed in water, its size slightly increased in parallel with the increasing charge ratio (+/−) (Fig. 4A), and a part of nanoplex was precipitated at a charge ratio (+/−) of 5/1 (data not shown). When NP-OH nanoplex was formed in NaCl solution, the presence of NaCl increased the size of the nanoplex. The size and ζ-potential of NP-OH nanoplex increased in parallel with the increasing charge ratio (+/−). NP-OH nanoplex was about 1 mm in size and became positive ζ-potential when formed at a charge ratio (+/−) of 3/1.

Next, we investigated the effect on size of nanoplex by incubation with culture medium (Fig. 4B). NP-OH nanoplexes formed in water increased the sizes at any charge ratios (+/−) after the incubation. In contrast, NP-OH nanoplexes formed in NaCl solution did not greatly change the sizes at charge ratios (+/−) of less than 3/1 after the incubation. NP-OH nanoplex was about 850 nm in size after the incubation when formed at a charge ratio (+/−) of 3/1. However, when NP-OH nanoplex was formed in NaCl solution at a charge ratio (+/−) of 4/1, the part of nanoplex was precipitated after the incubation.

Effect of Charge Ratio (+/−) of NP-OH/siRNA on Transfection Efficiency We examined the effect of various NP-OH/siRNA ratios on transfection efficiency to cells. Nanoplexes were formed at various charge ratios (+/−) in NaCl solution. NP-OH nanoplex at a charge ratio (+/−) of 1/1 slightly, and that of 2/1 moderately, and that of 3/1 strongly suppressed Gluc activity at 50 and 100 nM siRNA for 48 h after transfection (Fig. 5). In charge ratios (+/−) above 3/1, the suppression of Gluc activity seemed to be saturated, and was comparable to that of lipofectamine 2000. These results suggested that positively charged and/or large-sized nanoplex of siRNA could increase transfection efficiency in cells.

Cytotoxicity Next, we investigated cytotoxicity by transfection of NP-OH nanoplex to PC-3 cells by PI staining of cells. PI staining of the cellular nucleus was used as a marker for cell death 24 h after incubation of the cells with NP-OH nanoplexes. When formed at charge ratios (+/−) of less than 3/1, NP-OH nanoplexes did not actually exhibit cytotoxicity at 100 or 50 nM siRNA (Figs. 6A—C, F), but when formed at charge ratios (+/−) of above 4/1, the nanoplexes induced cytotoxicity at 100 nM siRNA (Figs. 6D, E). These findings suggested that NP-OH nanoplex formed at a charge ratio (+/−) of 3/1 has potential for efficient transfection of siRNA to cells with minimal toxicity; therefore, in subsequent experiments, we used 3/1 as the optimal charge ratio (+/−).

Dose Dependency of siRNA-Mediated Inhibition of Gluc Activity The persistence of gene silencing is a key factor when considering the therapeutic uses of siRNA. We thus studied the dose dependency of inhibition produced by NP-OH nanoplex 24 and 48 h after transfection into PC-3-Gluc cells. In the concentration of siRNA, NP-OH nanoplex formed in NaCl solution showed significant suppression of Gluc activity at above 50 nM Gluc siRNA compared with that of random siRNA (Figs. 7A, B). NP-OH nanoplex formed in water did not suppress Gluc activity for 48 h; however, that in NaCl solution exhibited strong suppression of Gluc activity, and this inhibition level increased with the increase of incubation (Figs. 7A, B).

Suppression of Bcl-2 mRNA and Protein by NP-OH Bcl-2 is one of the most important mammalian regulators of apoptosis and is overexpressed in the majority of human tumors, including the prostate.[22] We confirmed the decreased expression of bcl-2 protein by transfection of the NP-OH nanoplex of bcl-2 siRNA. NP-OH nanoplex of bcl-2 siRNA strongly inhibited the expression of bcl-2 protein at 100 nM siRNA 48 h after transfection, but did not affect the expression of β-actin (Fig. 8A). In contrast, EGFP and negative control siRNA did not affect the expression of both bcl-2 and β-actin proteins (Fig. 8A). Furthermore, we confirmed that the expression of bcl-2 mRNA decreased by 40—50% when NP-OH nanoplex of bcl-2 siRNA was transfected into the cells (Fig. 8B).